UPPSALA UNIVERSITET

Digital Comprehensive Summaries of Uppsala Dissertations from the Faculty of Medicine 1607

Towards Better Understanding of Etiological Mechanisms at the Neuromuscular Junction

EVGENII BOGATIKOV

ACTA UNIVERSITATIS UPSALIENSIS UPPSALA 2019

ISSN 1651-6206
ISBN 978-91-513-0791-6
urn:nbn:se:uu:diva-395581

Dissertation presented at Uppsala University to be publicly examined in The library of the Department of Clinical Neurophysiology, Uppsala University Hospital, entrance 85, 3rd floor, Uppsala, Wednesday, 11 December 2019 at 13:00 for the degree of Doctor of Philosophy (Faculty of Medicine). The examination will be conducted in English. Faculty examiner: Docent Viktorija Kenina (Department of Biology and Microbiology, Riga Stradins Universitet, Latvia).

Abstract

Bogatikov, E. 2019. Towards Better Understanding of Etiological Mechanisms at the Neuromuscular Junction. *Digital Comprehensive Summaries of Uppsala Dissertations from the Faculty of Medicine* 1607. 54 pp. Uppsala: Acta Universitatis Upsaliensis. ISBN 978-91-513-0791-6.

The neuromuscular junction (NMJ) serves as a model for understanding the mechanisms that determine communication between neurons and their target cells. Disorders of the NMJ can be either autoimmune or genetic (hereditary). The autoimmune disorder myasthenia gravis (MG) is caused by antibodies against the presynaptic nerve terminal or the postsynaptic muscle membrane, which make up the NMJ. The most common antibodies are directed against the acetylcholine receptor (AChR) or muscle specific tyrosine kinase (MuSK). An alternative to expand on preclinical *in-vivo* methods for studying mechanisms underlying diseases of neuromuscular transmission is to apply physiologic *in-vitro* models that would allow tissue-tissue as well as cell-cell interactions. A system that would allow cell-cell interactions in a biological fashion is the micro-electrode array (MEA) chip that allows co-culturing of motor neurons and muscle cells.

The primary hypothesis is that the suggested MEA can be used in creating a reliable model for healthy and diseased NMJ, allowing for manipulations and treatment assays. The secondary hypothesis is that small non-coding RNA, so called microRNAs (miRNA) have a specific role in neuromuscular transmission and in MG.

Study I demonstrated a method of long-term muscle cell culture on the MEA chips, which allows us to trace the development of muscle cells through the observation of their electrical activity at subcellular resolution. The maturation of skeletal muscle tissue was accompanied by a gradual increase in the amplitude and frequency of extracellular individual electrical spikes. The mature muscle tissue demonstrated the steady electrical activity with synchronized spike propagation in different directions across the chip.

Study II showed a specific upregulated profile of miRNAs in the muscles of MuSK antibody seropositive MG mice. Transfection of these miRNAs, miR-1933 and miR-1930, promoted downregulation of several proteins and further confirmation with qPCR revealed a specific blocking of IMPA1 and MRPL27, which are involved in intracellular signal transduction and mitochondrial biogenesis in skeletal muscles.

Study III revealed no correlation between the morphology of skeletal muscle cells and their electrical activity at an early developmental stage. However, the application of recombinant rat agrin increased the number of AChRs clusters in the culture of skeletal muscle and promoted a higher degree of spontaneous activity.

Keywords: Neuromuscular junction, Muscle cells, Microelectrode array, MicroRNA

Evgenii Bogatikov, Department of Neuroscience, Rostedt Punga: Clinical Neurophysiology, Ingång 85, 3 tr, Akademiska sjukhuset, Uppsala University, SE-751 85 Uppsala, Sweden.

ISSN 1651-6206
ISBN 978-91-513-0791-6
urn:nbn:se:uu:diva-395581 (http://urn.kb.se/resolve?urn=urn:nbn:se:uu:diva-395581)

List of Papers

This thesis is based on the following papers, which are referred to in the text by their Roman numerals.

I Lewandowska MK, Bogatikov E, Hierlemann AR, Punga AR. Long-Term High-Density Extracellular Recordings Enable Studies of Muscle Cell Physiology. *Front Physiol*. 2018;9:1424.

II Bogatikov E, Lindblad I, Punga T, Punga AR. miR-1933-3p is upregulated in skeletal muscles of MuSK+ EAMG mice and affects Impa1 and Mrpl27. *Neurosci Res*. 2019 pii: S0168-0102(18)30649-7.

III Bogatikov E. Punga AR. Evaluation of muscle action potential parameters in relation to morphology of skeletal muscle cell culture on high-density microelectrode array chips. *Manuscript.* 2019.

Contents

Abbreviations

ACh	Acetylcholine
AChE	Acetylcholinesterase
AChR	Acetylcholine receptor
AChR	Acetylcholine receptor
AP	Action potential
Atg9b	Autophagy-related 9B
ATP	Adenosine triphosphate
ATP	Adenosine triphosphate
BRCA1	Breast cancer 1
Brip1	BRCA1 Interacting Protein C-Terminal Helicase 1
cDNA	Complementary DNA
CFA	Complete Freund's adjuvant
CMS	Congenital myasthenic syndrome
CRD	Cysteine-rich domain
DHPRs	Dihydropyridine receptors
DIV	Days *in vitro*
DMEM	Dulbecco's Modified Eagle Medium
Dok-7	Tyrosine kinase-7
Dv1	Dishevelled receptor
EAMG	Experimental autoimmune myasthenia gravis
ECC	Excitation-contraction coupling
EPP	Endplate potential
EPP	Endplate potential
FBS	Fetal Bovine Serum
FGF	Fibroblast Growth Factor
Fz	Frizzled receptor
HBSS	Hanks' Balanced Salt Solution
HD-MEA	High-density microelectrode array
HPSCs	Human pluripotent stem cells
IgG	Immunoglobulin G
Impa1	Inositol monophosphate
Inpp5a	Inositol polyphosphate-5-phosphatase A
Lrp4	Low-density lipoprotein receptor-related protein 4
MEA	Microelectrode array
MG	Myasthenia gravis

miRNA	MicroRNA
MRF	Myogenic regulatory factor
MRF4	Muscle-specific regulatory factor 4
mRNA	Messenger RNA
Mrpl27	Mitochondrial ribosomal protein L27
MuSK	Muscle specific tyrosine kinase
Myf5	Myogenic factor 5
Myh8	Myosin heavy chain 8 (Myh8)
MyoD	Myoblast determination protein
myomiR	Muscle-specific miRNA
NADH	Nicotinamide adenine dinucleotide
NMJ	Neuromuscular junction
Pax	Paired box transcription factors
PBS	Phosphate-buffered saline
PCA	Principal component analysis
RR	Ryanodine receptor
SC	Satellite cell
SDH	Succinate dehydrogenase
SERCA	Sarcoplasmic/endoplasmic reticulum Ca^{2+}-ATPase pumps
Snn	Stannin
SR	Sarcoplasmic reticulum
T-tubules	Transverse tubular system
Tn-C	Troponin-C
Tn-I	Troponin-I
Tn-T	Troponin-T
VGCC	Voltage-gated calcium channel
VGSC	Voltage-gated sodium channel

Introduction

The neuromuscular junction

The neuromuscular junction (NMJ) is a cholinergic synapse where motor neurons interact with skeletal muscle fibers in order to regulate their contractile activity [1, 2]. The NMJ is composed of three zones that are distinguished both morphologically and functionally: the presynaptic part (motor nerve terminal), intrasynaptic part (synaptic basal lamina), and postsynaptic part (muscle membrane) [3] (Figure 1). Disruption of any part of the NMJ results in impaired neuromuscular transmission and in turn muscle weakness or even paralysis. To date, many diseases associated with impaired functionality of the NMJ have been described. Besides the heterogeneous group of congenital myasthenic syndromes (CMS) [4], that are associated with mutations in over 30 genes [5], other diseases are caused by an autoimmune attack of the NMJ, in particular myasthenia gravis (MG) [6]. Development of more specific treatment of such diseases requires a better understanding of the factors that normally determine the efficacy of NMJ transmission.

Since many decades, animal models have been crucial in determining the pathogenic role of the mutations and autoantibodies directed against the NMJ receptors, such as muscle specific tyrosine kinase (MuSK) [7, 8]. Passive immunization through repeated daily injections of immunoglobulin G (IgG) from MuSK antibody seropositive MG patients to rodents induce symptoms similar to human MG. In this case, administration of autoantibodies causes loss of synaptic function by suppressing the MuSK signaling pathway, which is essential for postsynaptic membrane differentiation [9].

However, the exact temporal mechanisms of the antibody attack at the NMJ are more difficult to elucidate in an MG animal model. Further, the phenotype of human neurodegenerative pathologies cannot be fully recapitulated in an animal model [10]. Despite the broad application of various *in vivo* models, the complex organization of the animal organism can also play a role as a limiting factor in unraveling the molecular mechanisms involved in the development of NMJ pathology. Alternatively, an *ex vivo* model can represent a powerful tool to study the role of specific molecules and compounds involved in functional organization of the NMJ in a defined and controlled system. Additionally, the development of *ex vivo* models significantly contributes to the reduction of animals used for drug screening in preclinical trials. Further, such an *ex vivo* model of the NMJ could in the long run take advantage of

humanized motor neurons and muscle cells in order to better model human disorders [10].

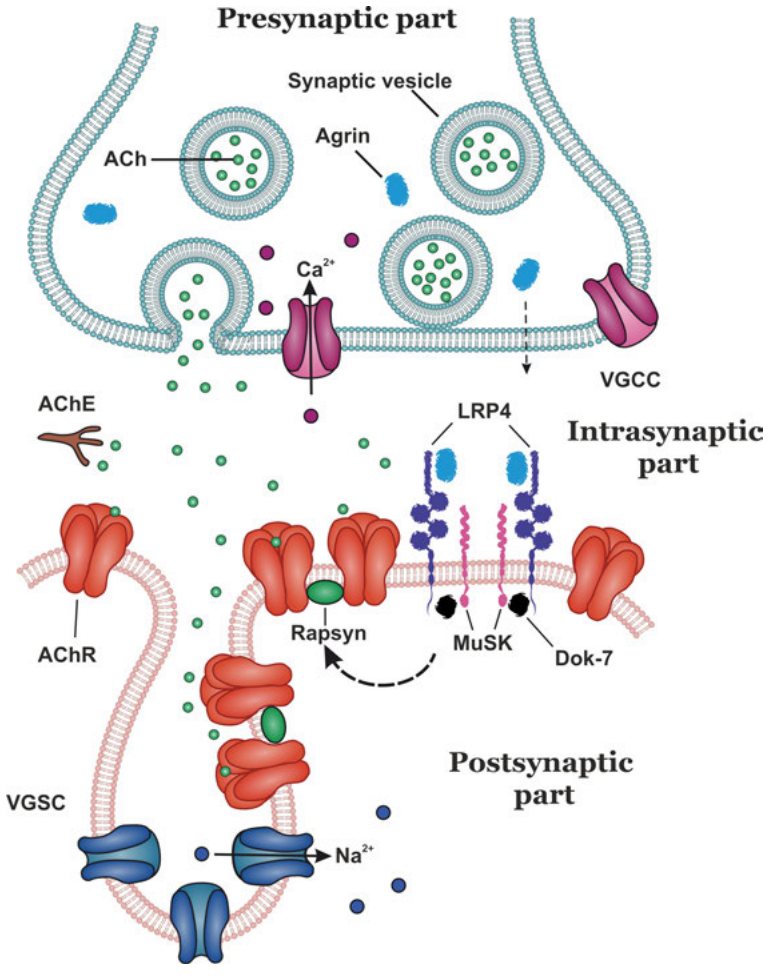

Figure 1. **Structure of the NMJ and key molecules involved in neuromuscular transmission as well as in NMJ diseases.** Upon the arrival of action potentials, voltage-gated calcium channels (VGCC) trigger the release of acetylcholine (ACh) from presynaptic vesicles of the motor neuron terminals. ACh crosses the synaptic basal lamina and binds to ACh receptors (AChRs), causing conformational changes that increase the permeability of the channel to cations. This results in depolarization of the postsynaptic muscle fiber via the opening of voltage-gated sodium channels (VGSC). ACh is then hydrolyzed by the acetylcholinesterase (AChE) in the intra-synaptic part. Agrin, released from the motor neuron terminals, binds to the low-density lipoprotein receptor-related protein4 (Lrp4), stimulating association between LRP4 and muscle specific tyrosine kinase (MuSK). This leads to increasing MuSK kinase activity and phosphorylation by tyrosine kinase-7 (Dok-7). The MuSK/Dok7 signaling complex promote downstream signaling pathway for AChRs aggregation, which also requires Rapsyn. Adapted from [3].

Organization and development of the NMJ

Motor neurons regulate skeletal muscle contraction through axons that enter the skeletal muscles. Axons divide into numerous branches to innervate individual muscle fibers. Each group of muscle fibers innervated by branches of the same motor neuron in the spinal cord is called a motor unit [11]. The motor axon terminal contains numerous synaptic vesicles, which all store the neurotransmitter acetylcholine (ACh) [12]. A fraction of these vesicles forms a readily releasable pool of ACh by docking at specific active zones on the presynaptic membrane. The active zones also contain transmembrane voltage-gated calcium channels (VGCC) mediating the fusion of synaptic vesicles with the presynaptic membrane.

Prior to the innervation by motor neuron axons, muscle fibers form primitive clusters of ACh receptors (AChR) in the central region during embryonal development; this developmental phenomenon is called muscle pre-patterning [13, 14]. Premature clustering of AChRs plays an important role in guiding the motor neuron axons. Further maturation of AChRs at the NMJ depends on factors released from motor neurons growth cones. The glycoprotein agrin is synthesized in motor neurons in a laminin-binding form, and released into synaptic basal lamina, where it induces postsynaptic differentiation, including AChR clustering [15, 16]. Neuronal agrin acts through phosphorylation of MuSK, which is involved in all aspects of NMJ development. MuSK is required for the pre-patterning of AChR clusters in embryonic myotubes [13] and further organization of the adult postsynaptic membrane [17]. However, agrin activates MuSK via binding to its co-receptor low-density lipoprotein receptor-related protein4 (Lrp4) [18, 19]. Lrp4 is a single-pass transmembrane protein with an extracellular region containing the binding sites necessary for assembling receptor complex between MuSK and agrin [20, 21]. Alternatively, MuSK can be activated in an agrin-independent manner by its interaction with the cytoplasmic adaptor downstream of tyrosine kinase-7 (Dok-7) [22, 23]. Dok-7 is exclusively expressed in skeletal and heart muscle and binds to the phosphotyrosine-binding site of MuSK [23]. Receptor-associated protein of the synapse (rapsyn) is another muscle membrane protein expressed from the early developmental stages, and involved in concentrating and anchoring of AChRs [24-27]. Rapsyn is associated with AChRs in post-Golgi vesicles, and is thus thought to play an essential role in directing transport vesicles to the postsynaptic membrane [28, 29]. Rapsyn binds tightly to AChRs to form a network with up to three rapsyn dimers contacting the cytoplasmic domain of each AChR molecule [30]. Moreover, rapsyn also binds to dystroglycan [31] and interact with a-actinin and b-catenin, which are important for stabilizing AChR clusters [32, 33].

Wnt signaling at the NMJ

Wnt is a family of cysteine-rich glycoproteins, which are crucial for diverse developmental processes [34] and that may also contribute to the NMJ formation [35]. The term Wnt derives from of the Drosophila gene wingless (wg) and the vertebrate gene Int-1 [36]. Wnt binding to Frizzled (Fz) and Lrp5/Lrp6 receptors on the plasma membrane results in the recruitment of the protein Dishevelled (Dv1) and the initiation of different downstream intracellular pathways [37-39]. Concerning NMJ, Wnt may signal through the extracellular cysteine-rich domain (CRD) of MuSK, which is homologous to that in the Fz receptor [40]. MuSK also interacts intracellularly with Dvl, which regulates agrin-induced AChR clustering [41]. Deletion of the CRD in mice impairs NMJ formation through a drastic decrease in the number of pre-patterned AChR clusters [42, 43]. In cultured C2C12 muscle cells, some Wnts can promote AChR clustering in the absence of agrin (Wnt9a, Wnt9b, Wnt10b, Wnt11, and Wnt16) or increase the number and size of AChR clusters induced by agrin (Wnt3) [44-46]. On the contrary, Wnt3a inhibits agrin-induced AChR clustering through suppression of rapsyn expression [47]. In addition, in mutant mice lacking or overexpressing β-catenin, a key mediator of the canonical Wnt pathway, both pre- and postsynaptic deficiency is observed in muscle fibers [48-50].

Skeletal muscles

Skeletal muscles make up the most abundant tissue in the body of vertebrates, accounting for about 40% of the total human body weight [51]. The basic function of skeletal muscle is contraction, which enables the various movements necessary for physical activity. Skeletal muscles also contribute to the maintenance of basal energy metabolism, acting as a reservoir for amino acids or carbohydrates, and generating heat during shivering or physical activity [51, 52].

Skeletal muscles of mammals are heterogeneous and differ in their contractile properties. This heterogeneity is determined by several motor units assembling into muscle fibers and that allows each muscle to respond in the best way to functional requirements, from continuous activity with low intensity to fast and strong maximum contractions. Several classification schemes have been developed to describe types of muscle fibers with distinct movement rates, response to neural inputs, and metabolic processes [53]. Based on expression of myosin isoforms, velocity of contraction and resistance to fatigue, skeletal muscle fibers can be broadly classified on slow-twitch fibers (also called ST or type 1), fast-twitch oxidative-glycolytic fibers (FOG or type 2A), and fast-twitch glycolytic fibers (FG or type 2X) [54]. The type 2X have been identified in the muscles of small mammals but not in humans [55]. Fast-

twitch muscle fibers, usually white, are less dependent on oxidative metabolism and utilize anaerobic pathways. Slow-twitch muscle fibers are fatigue resistant and have a large capillary network with much myoglobin, a red oxygen-binding protein involved in the delivery of oxygen to the mitochondria. The large amounts of myoglobin provide the characteristic red color to slow-twitch muscle fibers [52].

Skeletal muscles of mammals possess a high adaptive potential to physiological demands, such as growth or injury. The best known example of such adaptation is muscle hypertrophy in response to resistance exercise training, which is generally characterized by an increase in muscle strength and muscle mass [56-58]. In contrast, acute muscle injuries, muscle disorders, immobilization as well as aging can result in significant muscle atrophy and loss of function [59, 60]. This in turn may cause severe impairment of everyday activities and thus reduced quality of life. In this sense, a better understanding of the developmental basis of skeletal muscle, their functions and regeneration process can help to find novel therapies to treat muscle diseases. In contrast, cardiac and visceral smooth muscles are intrinsically active and do not require neural initiation of activation. However, these muscles are innervated and their activity is modulated by nerves and sometimes by humoral factors. These different types of control are broadly classed as voluntary and involuntary [52].

Myogenesis

Development of skeletal muscle, myogenesis, can be divided into several distinct phases: 1) transformation of multipotent progenitors into myoblasts; 2) fusion of myoblasts and differentiation into multinucleated primary myotubes; 3) myotubes differentiation into muscle fibers upon innervation and 4) maturation of muscle fibers and their bundling into functional muscles [2, 61-64].

Myogenesis is controlled by a vast network of transcription factors, including members of the paired box (Pax) family proteins. The Pax family of transcription factors play key roles during tissue specification and organ development [65]. In the context of myogenesis, Pax3 and Pax7 are important upstream regulators of muscle formation. Pax3 is expressed in muscle progenitor cells at the earliest stages of embryogenesis and regulate expression of other myogenic regulatory factors (MRFs) [66]. MRFs coordinate the activity of many genes involved in muscle cell differentiation and include four genes: myogenic factor 5 (Myf5), muscle-specific regulatory factor 4 (MRF4), myoblast determination protein (MyoD) and myogenin [67]. Myf5 and MyoD are critical factors required for skeletal muscle lineage determination in the embryos [68], whereas myogenin is important for the terminal differentiation of committed myoblasts into muscle fibers [69]. Mrf4 has a dual role acting as a differentiation gene in postmitotic myoblasts, but it can also determine myogenic identity in the absence of Myf5 and MyoD [70].

Once myogenesis is completed, undifferentiated myogenic cells form a pool of muscle stem cells residing within the muscle fiber [71]. These cells are located along the outer boundary of the muscle skeletal membrane like satellites (Figure 2), and therefore named satellite cells (SCs) [72].

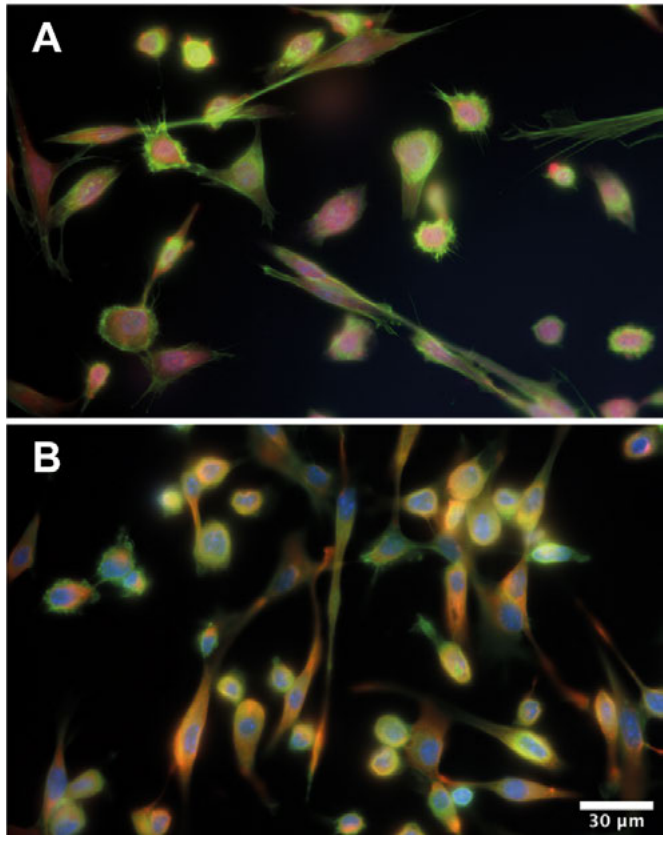

Figure 2. **Primary culture of myoblasts stained for muscle specific markers: A.** MyoD1 (red), F-actin (green) and Dapi (blue); **B.** Desmin (red), F-actin (green) and Dapi (blue)

Under normal physiological conditions, most SCs remain in a quiescent undifferentiated state and express the transcription factor Pax7 [73]. Upon acute muscle injury or in different disease states, quiescent SCs become activated and re-enter the myogenic cycle, giving rise to a new generation of myoblasts, which later differentiate into muscle fibers and have the potential to repair damaged muscle [74, 75]. The myoblasts withdraw from the cell cycle, adopt a spindle shape, and align with each other, forming a braid, and the fusion occurs. The possibility to isolate and culture satellite cells obtained from the muscles of various organisms, including humans, allows creation of *in vitro* models for studying neuromuscular diseases.

Structure of the mature skeletal muscle

Skeletal muscles consist of elongated muscle cells, also known as muscle fibers, which are highly specialized multinucleated cells surrounded by a cell membrane, the sarcolemma [76]. The presence of multiple nuclei ensures adequate proteins synthesis and degradation along the entire length of the muscle fiber [77]. Each muscle fiber contains several hundred to several thousand myofibrils; each myofibril is in turn composed of many filaments. [78]. These filaments are partially adjacent to each other and represented by two main varieties: the thin filament and the thick filament. The major constituent of the thin filament is actin, whereas the main component of the thick filament is myosin [77]. The highly organized arrangement of these filaments into repeating contractile structures, called the sarcomere, underlies the striated appearance of skeletal muscle. The sarcomere is a very dynamic structure and requires multiple regulatory proteins bound to myosin and actin filaments (Figure 3).

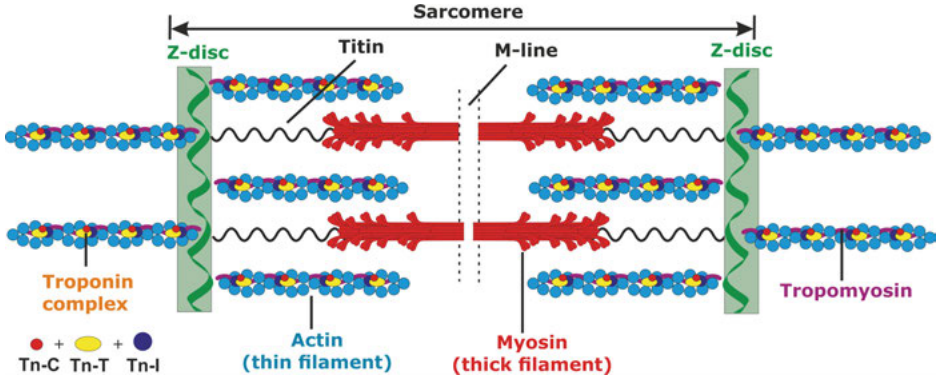

Figure 3. **Schematic representation of a skeletal muscle sarcomere.** Each titin molecule (black) extends from the Z-disk (green) to the M-line. Part of the titin molecules are closely associated with the myosin thick filaments (red). The actin filaments (cyan) are wrapped by tropomyosin (purple). Adapted from [78]

The actin filaments are made up of two chains that form a long double helix. Tropomyosin molecules are wrapped spirally around this helix [79, 80] and form regulatory complex with three subunits of troponin: troponin-C (Tn-C), troponin-T (Tn-T), and troponin-I (Tn-I) [76, 81]. Each of the three troponin subunits has a unique function: Tn-T binds the troponin components to tropomyosin, Tn-I inhibits the interaction between the thick and thin filaments, and Tn-C contains the binding sites for the Ca^{2+}[81].

The myosin filament is a complex protein molecule, which consists of two globular heads attached trough a flexible link to a long tail [77]. The flexible link allows the heads part to form the cross-bridges with the thin filament, actin. These heads contain an actin-binding site and a catalytic site hydrolyzing adenosine triphosphate (ATP) [81]. Interactions between myosin heads

and actin are regulated through Ca^{2+} binding to tropomyosin-troponin complex [82, 83]. In low Ca^{2+} conditions, tropomyosin covers the external domain of actin and blocks the myosin-binding site. In the presence of high calcium concentration, Tn-C binds calcium and mediates dissociation between Tn-I and tropomyosin. This leads to a conformational shift of tropomyosin, which then exposes binding sites on actin for the myosin head domains [84-86].

In addition to proteins directly involved in the contraction process, several other important proteins are required for the structure and function of sarcomeres. For instance, the thick filaments contain titin, a giant elastic protein that act as a framework holding the myosin filaments in the center of the sarcomere [87]. Nebulin is another filamentous protein that extends along the thin filament length and playing scaffolding role for actin filaments [87, 88].

At regular intervals, the sarcolemma forms perpendicular invaginations into the muscle fiber, creating a network of the transverse tubular system (T-tubules) inside the cell. The T-tubules are adjacent to the sarcoplasmic reticulum (SR), a closed organelle wrapping myofibrils and containing high concentrations of Ca^{2+}. This two-membrane system regulates rapid changes in myoplasmic free Ca^{2+} concentration. The T-tubule has L-type voltage-sensitive Ca^{2+} channels named dihydropyridine receptors (DHPRs) that are mechanically linked to Ca^{2+} channels in the SR named ryanodine receptor (RRs) [89].

Excitation-contraction coupling and skeletal muscle contraction

In the context of skeletal muscle physiology, the term *contraction* is associated with shortening of the muscle fiber, although it actually refers to activation of the muscle [52]. Excitation-contraction coupling (ECC) refers to the sequence of events in which depolarization of the sarcolemma leads to a mechanical contraction.

The motor neuron receives various signals from the corticospinal pathways, ranging from the anterior horn of the spinal cord to the motor cortex of the brain [90]. Excitatory signals results in depolarization of the motor neuron and the formation of the action potential (AP). APs are rapid transient changes in membrane potential that results from an increase in ionic conductance of the cell membrane [91]. The AP can move from one area of the cell membrane to another and so it can be used to signal between different neurons or their target cells. The process of neuromuscular transmission includes forwarding APs from the motor neurons through motor axon terminals to the postsynaptic membrane of the skeletal muscles [90].

The arrival of the AP to the motor axon terminal opens VGCC, significantly increasing the concentration of cytoplasmic Ca^{2+} in the vicinity of the active zones, followed by activation of the molecular machinery (SNARE family) that orchestrate exocytosis of the synaptic vesicles [92]. Once vesicles fuse with the presynaptic membrane, ACh molecules release

into the synaptic basal lamina, where they bind to the muscle AChRs, localized at high density in deep junctional folds of the muscle membrane [3]. This high density of junctional folds ensures reliable neuromuscular transmission. Together, the multiple ACh quanta released by a neuronal AP open thousands of AChRs, and the resulting net influx of positive charge causes a local depolarization of the postsynaptic membrane, the endplate potential (EPP). The EPP activates voltage-gated sodium channels (VGSCs), which are highly concentrated in the junctional folds [93]. This further creates an influx of Na^+ ions and the spread of the AP along the muscle fiber, triggering muscle contraction. The duration of the EPP is a few milliseconds and is terminated when ACh becomes degraded by the enzyme acetylcholinesterase (AChE) that is located in the synaptic basal lamina [3].

The AP propagates not only longitudinally but also radially down to the T-tubules, depolarization of which leads to conformational changes of the DHPRs with following activation of RRs and release of Ca^{2+} from the SR into the cytosol. The released Ca^{2+} can bind to the myofilaments and activate cross-bridge cycling, before the sarcoplasmic/endoplasmic reticulum Ca^{2+}-ATPase (SERCA) pumps on the SR membrane remove Ca^{2+} back into the SR. During the relaxation of skeletal muscle, SERCA pumps remove cytosolic Ca^{2+} from the myofilaments and restore the SR to its resting state [94, 95].

Methods of assessing muscle electrical activity

Skeletal muscle contraction relies on the ability of muscle fibers to generate the membrane potential by dynamic ion exchange with the extracellular environment through membrane channels and pumps [96]. For this reason, the measurement of ion movements is instrumental in investigating skeletal muscle physiology. A wide range of electrophysiological approaches has been applied to measure changes in membrane potential and current produced by transmembrane ion movements in excitable tissues such as skeletal muscle [97-101].

The basis of electrophysiological measurements is the creation of contact between electrical tissue or electrical cells and an electronic recording unit. Electrical contact is achieved using an electrode and an electrochemical half-cell, which consists of a solid (metal) conductor and an electrolyte [102]. Depending on the location of the electrodes relative to the measured object, the electrophysiological recordings are divided into intracellular or extracellular.

Intracellular recording involves inserting an electrode into the cell and measuring voltage and / or current through the cell membrane with respect to an extracellular reference electrode. The most famous example of intracellular measurements is the patch-clamp method, which allows for a very accurate assessment of the electrical activity of a single cell [103]. However, this method requires sufficient stabilization and tight contact between the

electrode and the investigated cell and therefore can not be implemented for clinical electrophysiological studies on nerves and skeletal muscles in humans.

Clinical electrophysiological assessment requires extracellular recordings that measure the field potential outside of cells. Measurement of muscle contraction can be performed by both invasive and noninvasive methods and is called electromyography (EMG). Surface EMG is the main non-invasive method in which two electrodes in the form of small round metal disks are placed on the skin overlying the muscle. This method is very sensitive to external electromagnetic interference and also to other sources of noise, and therefore requires stable electrical contact between electrodes and skin [104]. For direct measurement of electrical activity, a variety of transdermal needle electrodes are available. The most common type is the concentric needle electrode made of platinum or silver thin wire, and which is mostly insulated, except at its tip [105]. During measurement, this electrode is inserted into a muscle and must be used in conjunction with a reference electrode in order to form a closed electrical circuit. The firing of APs results in the transient opening of the sodium channels and the influx of sodium ions down its concentration gradient into the cell. This reduction of positive ions from the extracellular space near the tip of the recording electrode can be measured as a negative transient voltage fluctuation with respect to the reference electrode [106]. These APs in the form of transmembrane ion fluxes are amplified and displayed on the screen of the oscilloscope and fed through a loudspeaker, so they can be monitored by ear.

Disorders of the neuromuscular junction

Congenital myasthenic syndromes (CMS)

The heterogeneous disorders caused by mutations in genes coding for proteins at the NMJ are named congenital myasthenic syndrome (CMS) [3]. To date, mutations in at least 30 genes related to the development of CMS have been described [4, 5]. The CMS classification is depending on the location of the mutant protein and can be as presynaptic, intrasynaptic and postsynaptic [3].

Presynaptic CMS are usually associated with mutations in CHAT, the gene encoding choline acetyltransferase, responsible for ACh synthesis [107]. The disease typically causes episodes of hypotonia, bulbar paralysis, and apnea at birth. Symptomatic treatment involves inhibition of AChE activity and application of 3,4-Diaminopyridine, blocking potassium channel efflux in nerve terminals so that AP duration is increased [108]. The most common form of postsynaptic CMS is related to mutations in the genes encoding subunits of the muscle form of nicotinic AChR (~60%) [3]. These mutations can be divided into two major groups: mutations altering the kinetic properties of

AChRs, and mutations effecting on expression level of AChRs [4]. For instance, mutations of genes encoding rapsyn or MuSK dramatically influence agrin-MuSK-LRP4-mediated clustering of AChR, which resulted in multiple and dispersed synaptic contacts over the fiber surface [109-111].

Myasthenia gravis (MG)

Epidemiology and diagnosis

Myasthenia gravis (MG) is an autoimmune disorder characterized by the presence of antibodies against postsynaptic proteins of the NMJ resulting in weakness and fatigue of skeletal muscles [6, 112]. The muscle fatigue can be localized or generalized, with a tendency of worsening with repetitive muscle use or physical exercise. The weakness typically affects ocular, bulbar and proximal extremity muscles, and as a rule with symmetrical location, except of eye muscles involvement, which is often asymmetric [6]. The prevalence of MG is 150 to 250 cases per 1 million, with an annual incidence of 8 to 10 cases per 1 million individuals [113].

Serum antibodies affecting the neuromuscular transmission are important markers in establishing the diagnosis of MG. Approximately 80% of patients with generalized MG have autoantibodies against the nicotinic AChRs [114, 115]. Antibodies against MuSK are found in around 5-10% of patients with AChR antibody seronegative MG [116]. LRP4 antibodies are present in approximately 15% of MG patients who are AChR/MuSK antibody seronegative [117]. Patients without detectable antibodies against any of these three major receptors are referred to as seronegative. The ultimate diagnosis of MG is made by a combination of objective clinical symptoms of muscle fatigue, detectable serum antibodies and signs of disturbed neuromuscular transmission on neurophysiological examinations (repetitive nerve stimulation and/or single fiber electromyography). Individualized treatment depends on antibody subtype, the disease severity and the age and sex of the patient [118]. In case of MuSK antibody seropositive (MuSK+) MG, the severity of disease correlates with the titer of serum MuSK antibodies, which can facilitate diagnosis and probably also improve the treatment of these subgroups of patients [119, 120]. However, the majority of patient belongs to the subgroup of AChR antibody seropositive (AChR+) MG, where no correlation has been shown between AChR antibody concentration and disease severity [119].

Pathogenic antibodies and treatment in MG

The AChR antibodies mainly belong to the IgG1 and IgG3 subclasses and can bind to a variety of epitopes on AChRs. There are three main mechanisms by which these autoantibodies negatively act on NMJ transmission: 1) blocking the binding site of AChRs to ACh, thereby preventing neuromuscular transmission; 2) cross-linking AChRs, which induces accelerated internalization

and degradation of AChRs; and 3) activation of the complement cascade, leading to damage postsynaptic membrane at the NMJ [6, 114, 121]

MuSK antibodies are produced almost exclusively by regulatory B cells of IgG4 isotype. The injection of Musk IgG4 antibodies, but not IgG1-3, disrupts both presynaptic and postsynaptic parts and reduced AChR clustering in the NMJ [122-124]. The main function of the MuSK antibodies is to disrupt the interaction between MuSK and Lrp4 [125].

Lrp4 antibodies block the interaction between agrin and LRP4 and thereby prevent AChR clustering. Moreover, LRP4 antibodies belong to the IgG1 subclass and therefore can induce complement-binding [126].

All MG therapies are designed to moderate the disease severity and include symptomatic drug treatment and immunosuppressive pharmacological treatment [6, 127]. The symptomatic treatment typically consists of AChE inhibitors that render more ACh available at the NMJ, for example pyridostigmine bromide. Immunosuppressive therapy targets the autoimmune dysregulation of the disease, and can be divided into chronic or acute treatment. Chronic therapies include corticosteroids, cyclosporine, azathioprine, which all reduce the number of available T and B cells. More modern immunosuppressive treatment includes for example Rituximab. Acute treatment has to be initiated in case of severe disease worsening, in particular so called myasthenic crisis that results in respiratory muscle weakness and includes plasma exchange and intravenous immunoglobulins that quickly reduces the number of circulating antibodies. For patients with AChR antibodies and those with a thymoma, thymectomy is recommended as treatment due to the involvement of thymus in directing T cells.

MicroRNAs

There is a great need for reliable objective biomarkers to monitor the disease course in MG and microRNAs have arisen as potential biomarkers. [128] MicroRNAs (miRNAs) are short non-coding RNA sequences, ~22 nucleotides, capable of silencing target genes by binding to target messenger RNAs (mRNAs) which results in post-translational protein inhibition. Therefore, miRNAs act as negative regulators of gene expression and have been implicated in many biological processes, including development and tissue maintenance [129]. Many miRNAs are ubiquitously expressed in most tissue and cell types, while others were defined as tissue-specific whose expression is 20-fold or higher compared with the mean of the other tissues [130]. Therefore, these circulating extracellular miRNAs that are available for quantitative analysis in most biofluids such as blood, have emerged as attractive diagnostic and prognostic biomarkers of disease. Circulating miRNAs fulfill the requirements for biomarkers, as they can be detected and quantified with high sensitivity and specificity in various biological fluids that are easily accessible through

routine clinical sampling. Furthermore, the high stability of miRNAs in body fluids and the relatively low-cost detection methods favor the use of circulating miRNAs as biomarkers [131, 132].

The role of intracellular miRNAs in skeletal muscle physiology

Muscle-specific miRNAs are called myomiRs and so far eight miRNAs have been defined to be specifically important in muscle tissue: miR-1, miR-133a, miR-133b, miR-206, miR-208a, miR-208b, miR-486 and miR-499 [133]. MyomiRs are expressed in both cardiac and skeletal muscle with the exception of miR-206, which is skeletal muscle-specific, and miR-208a, which is cardiac muscle-specific [134]. Several miRNAs can be involved in the maintenance of satellite cell quiescence. For instance, miR-489 is highly expressed in quiescent satellite cells and remarkably downregulated following activation [135]. Another miRNA, miR-31 maintains quiescence state of satellite cells by downregulation of Myf5 mRNA. Upon activation of satellite cells, messenger ribonucleoprotein granules collapse, leading to degradation of miR-31 and releasing Myf5 transcripts with following accumulation of the Myf5 protein and initiation of myogenesis [136].

Moreover, upon muscle injury, the expression of miR-1 and miR-206 is also remarkably decreased. This reduction correlates with activation of satellite cells and their transition from quiescence to proliferation state. Later, both miRNAs accelerate myogenic differentiation by suppressing Pax3 and Pax7, which consequently results in increased activity of MyoD [137, 138]. In contrast, miR-133 enhances myoblast proliferation by repressing the serum response factor, which is involved in myogenic differentiation and expression of actin cytoskeleton genes [139-141]. Additionally, miR-221 and miR-222 also promote myoblast proliferation by targeting the cell cycle inhibitor p27 and the differentiation factor myogenin [142]. Moreover, miRNAs can be useful as a novel therapeutic strategy for muscle injury. For instance, simultaneous injection of miR-1, miR-206 and miR-133 into skeletal muscle following injury resulted in the up-regulation of myogenic markers myogenin, MyoD and Pax7, promote myotube differentiation and significant fibrosis prevention [143]. Overall, myomiRs are crucial regulators of skeletal muscle physiology and could be considered as future treatment targets.

Circulating extracellular miRNAs in neuromuscular diseases

In addition to their well-characterized intracellular accumulation, miRNAs can also be detected in the extracellular space in almost all biofluids. Exosome mediated transfer of mRNAs and miRNAs are a novel mechanism of genetic exchange between cells [144]. Although the exact role of circulating miRNAs is not yet fully understood, multiple studies have revealed that fluctuations in the level and composition of extracellular miRNAs may reflect the course of

different diseases, such as cancer [131]. The imbalance of circulating myomiRs has been described in patients with various skeletal muscle disorders. For example, patients with Duchenne´s muscular dystrophy have elevated serum levels of the myomiRs miR-1, miR-133, miR-206 [145], as well as miR-208a, 208b, and miR-499 [146]. These findings indicate that circulating miRNAs might even be considered as diagnostic tools for detection of skeletal muscle pathologies. Moreover, circulating miRNAs seem to have a disease-specific profile in MG [128]. Recent studies in AChR+ MG revealed elevated levels of the immuno-miRNAs miR-150-5p and miR-21-5p; in particular miR-150-5p levels were lower in immunosuppressed patients and in patients with clinical improvement following thymectomy [147, 148]. In the other immunological subtype of MG, MuSK+ MG, another profile of circulating miRNAs was found, including upregulation of the let-7 family of miRNAs (let-7a-5p and leg-7f-5p) as well as miR-151-5p and miR-423-3p [149].

In vitro models of skeletal muscles

Multiple skeletal muscle models have been applied for regenerative therapy [150], fundamental biological research [151] and drug testing [152, 153] as well as for patients with injured, diseased, and age-related muscle dysfunction [154, 155]. One of the most important characteristics of skeletal muscles is their ability to generate contractile force. Thus, artificial skeletal muscle models should imitate the architecture of native muscles and demonstrate contraction.

However, non-innervated human skeletal muscle cultures, unlike various skeletal muscle cells of animal origin, do not exhibit spontaneous contraction or form differentiated postsynaptic components of NMJ when cultured under standard conditions *in vitro* [156, 157]. Skeletal muscle cells of animal origin display a more advanced level of postsynaptic organization than human cells, which lack basal lamina [158] and diffusely express AChE [157] and nAChRs [157, 159]. In contrast, clusters with high concentration of nAChRs are often present in non-innervated cultured embryonic chick [160], rat [161] and mouse [162] myotubes. Cultured mouse myotubes display highly developed nAChR clusters [163] and may contract independently of innervation by motor neurons [164].

In addition to a variety of primary skeletal muscle cell culture models, a significant bulk of research has also been done using cell lines, such as the C2C12 cell line [165]. This cell line is a subclone derived from C2 myoblasts that were originally developed in 1977 to study muscular dystrophies *in vitro* [166]. Since they have a high division rate, homogeneity and are easy to culture, C2C12 cells provide a robust and reproducible system. Therefore, C2C12 cells are used for studies of the cell cycle [167], myogenic differentiation [168, 169] and myomiRs [170]. C2C12 cells fuse into

multinucleated myotubes when exposed to low-serum medium, express highly differentiated nAChR clusters [163] and spontaneously contract [171, 172]. However, C2C12 myotubes are generally not suitable for long-term culture experiments, because they often detach from the cell culture surface after 7 to 10 days due to spontaneous contraction [173, 174]. Moreover, the contractile proteins present in these cells do not completely mimic muscle fibers *in vivo*, since they are usually disorganized and rarely form aligned sarcomeres [175, 176].

Models of MG: experimentally induced autoimmune MG

The main aim of experimental autoimmune MG (EAMG) is to investigate the pathological mechanisms of the disease and to propose potential new therapies in order to replace the current unspecific immunosuppressive treatment strategies. Different immunosuppressants are ineffective in some MG patients and cause a range of side effects. Therefore, new therapeutic approaches are needed [177].

Animal models for MG

EAMG models are based on active or passive induction of disease primarily in rodents. These well-established models share many clinical and electrophysiological features with MG in humans, including the presence of AChR or MuSK antibodies in serum, reduced postsynaptic response to repetitive nerve stimulation, and the loss of muscle AChRs [178]. Animals with EAMG develop muscle weakness and fatigue. Two basic approaches are used to induce antibody-mediated MG in animals. The passive transfer model of MG involves injection of antibodies derived from patients with MG or from AChR immunized animals in the chronic phase of EAMG. This does not include any activation of the animals own immune system. The other strategy, actively induced EAMG, is induced by injection of purified protein, either AChR, MuSK or Lrp4 in adjuvant, triggering the production of antibodies to these receptors [178]. Myasthenic symptoms typically appear after the first or second injection of recombinant extracellular domain of MuSK in complete Freund's adjuvant (10–30 μg), Mice with MuSK+ MG demonstrate decrease in body weight, muscle strength and reduced compound motor AP at repetitive nerve stimulation. These symptoms are due to the fragmentation of the AChR clusters of the NMJ into multiple small AChR clusters, with the subsequent loss of AChRs [9].

Cell culture models for MG

Primary muscle cells derived directly from animals or their alternative muscle cell lines are often used for modeling MG. Cultured myotubes express the membrane proteins involved in the NMJ development and that also constitute the objects for antibody mediated attack in MG. Indeed, plasma or IgG from

MuSK+ MG patients can inhibit the formation of AChR clusters and/or cause disassembly of pre-existing AChR clusters in cultured myotubes. Moreover, experiments on cultured muscle cells helps to shed light on postsynaptic mechanisms in both AChR forms and MuSK antibodies in MG [9].

Multiple studies have focused on the application of various *in vitro* co-culture systems in which motor neurons are grown together with muscle cells, in order to investigate the mechanism of the formation and possible destruction of the NMJ. The simplest approach is to culture motor neurons on the surface of muscle cells, leading to the formation of rudimentary NMJs [179]. However, such systems do not allow for reconstitution of more physiological conditions, which implies also the spatial separation between muscle tissue and somas of motor neurons located in the spinal cord. In addition, such conditions exclude site-specific experimental treatment directed exclusively to the motor neuron soma or just the axon. Compartmented microfluidic chambers have been designed to overcome these problems, allowing spatial and physiological separation between motor neurons and muscle cells [180]. The basic idea of cell culture in microfluidic systems comprises application of two- or more fluidically isolated culture chambers connected by microchannels, the size of which does not allow cell bodies to enter the adjacent reservoir. At the same time, neurons are able to direct their axons towards the neighboring chamber by microchannels in response to the growth factors present there. For instance, motor neuron cultured in microfluidic system extend axons through the separating microchannels to the distal chamber and are capable of inducing AChR clustering on primary myotubes, and NMJ formation [181].

Microelectrode array: novel muscle model system

In addition to spatial modeling, electrophysiological characterization of NMJs also contribute to our understanding of pathogenic mechanisms involved in development of neuromuscular disorders. Besides intracellular recordings using the patch-clamp technique, which have enabled the study of single cells, ion channels, as well as cell to cell communication and connectivity, modern electrophysiology have an advantage in the form of microelectrode arrays capable now of monitoring the activity of many cells at once. Microelectrode matrices (MEA) allow studying the physiology of the network since they are designed for the simultaneous recording of extracellular signals from many excitable cells. Beginning with application of 30-electrode arrays for *in vitro* extracellular measurement of heart cells [182], the development of MEA technology has led to the establishment of high-density microelectrodes array chip with more than 3000 electrodes per mm^2, which allows for monitoring electrical activity of large cell network at subcellular resolution [183, 184]. Moreover, MEA technology can be integrated with microfluidic systems to form multiple compartment MEA-devices [185, 186]. This can significantly improve application of cell culture modeling for study the development and maintenance of the NMJ, different muscular pathologies and drug screening.

Aims

The general aim of this PhD project is to develop an NMJ disease model *in vitro*, which allows for specific manipulations that are not possible to perform *in vivo*.

The proposed projects also aim at providing new insights to the NMJ in health and disease, for example regarding the regulation of miRNA.

Hypotheses

I. The primary hypothesis is that the high-density MEA chip can be used to create a reliable model for diseases of the muscle and NMJ, allowing for detailed manipulations and treatment assays.

II. The secondary hypothesis is that small non-coding RNA (especially miRNA) has a specific role in neuromuscular transmission and in MG.

III. The third hypothesis is that the muscle fiber diameter positively correlates with muscle AP amplitude and that agrin application induces AChR clustering and increased electrical activity.

Methods

Ethics

The animal ethics committee of Uppsala has approved the passive transfer MG model in mice (Dnr C41/15) as well as collection and culture of motor neurons and muscle cells from rodents (Dnr C97/15).

Study I

Primary myoblast culture

Primary myoblasts were obtained from the limbs of post-natal day 1-3 mice. Neonatal pups were sacrificed by decapitation, skin was removed, and all four limbs were excised and placed into sterile Hanks' Balanced Salt Solution (HBSS). Muscles were dissected from bones and intensively minced into small pieces before enzymatic digestion for 1 h in collagenase-dispase solution supplemented with 2mM $CaCl_2$. Enzymatically digested muscles were triturated by pipetting with 1 mL plastic tip. After centrifugation, cells were re-suspended in F-10 based growth medium supplemented with 10% Fetal Bovine Serum (FBS), 2.5 ng/ml of Fibroblast Growth Factor (FGF) and 1% penicillin-streptomycin. Cell suspension was pre-plated in non-coated plastic Petri dishes for 30 minutes. This step reduces the number of non-specific cells, like fibroblasts. After that, non-adherent cells, including myoblasts, were plated in collagen-coated T75 flasks. These cells were kept in growth medium for a few days at 37˚C and 5% CO_2. Upon achieving about 70% confluency cells were detached using Phosphate-buffered saline (PBS) and 0.05 trypsin-EDTA and split. In order to purify the myoblast from presence of fibroblasts, cell culture was pre-plated prior to plating in the new flasks. After enriching for myoblasts in this manner for about one and a half week, myoblasts were plated with a density around 250-300k/mL onto high-density microelectrode array (HD-MEA) chips, which had previously been sterilized and treated with polyethyleneimine for one hour and mouse laminin for one hour. Cells were kept in proliferation medium for another two days and then switched to differentiation medium (Dulbecco's Modified Eagle Medium (DMEM) containing 5% horse serum and 1% penicillin-streptomycin).

High-density Microelectrode Array Chip

The design, fabrication, and characterization of the HD-MEA can be found elsewhere [187].The relevant features for the present work are as follows: 3.85 × 2.10 mm^2 array of 26,400 bright Pt working electrodes with a pitch of 17.5 μm; 1024 reconfigurable readout channels; on-chip filtration, amplification and digitization at 20 kHz, on-chip counter electrode, and 32 stimulation units.

Electrophysiological Recordings

All measurements of the electrical activity of myotubes began a few days after seeding of cells and were carried out using a series of 26 random configurations, with 1024 different electrodes per each configuration and for 20-60 seconds.

The electrodes with the largest spikes were selected as electrodes of interest and were used to create spontaneous triggered profiles. These electrodes of interest (10-30) remained fixed in all configurations, while the others 1000 channels were directed to random electrodes. From 26 to 32 of these configurations were created for efficient sampling of the entire chip, lasting from 20 to 60 seconds each.

Data Analysis

Data analysis was performed in Matlab using custom software. Spike detection and rudimentary spike sorting were performed offline.

Spike detection and sorting

The spike detection was performed using the amplitude thresholding method when all spikes exceeding a threshold of six standard deviations were first identified and isolated and then combined into complex spikes. These spikes were sorted by using principle component analysis (PCA) in Matlab. Spikes sorting into several groups was performed based on very similar shapes or using template matching.

Triggered spontaneous scans

Triggered spontaneous profile was applied in order to find information about how individual spikes propagate over electrode array within certain time window. All signals observed over many configurations on an electrode of interest were sorted out and the most common spike was then chosen. The timing information associated with this spike were used to find traces from all other configurations on all of the other electrodes, were then cut out within a chosen window ±2 – 5 ms, with a trigger provided by the spiking of the cell of interest.

Template matching

Template matching was used to find all the spikes corresponding to the selected profile and extract optimal time information. After PCA a template was created for each group by averaging all the spikes observing within the group.

Spike propagation profiles

Raster plots were converted into histograms by choosing an appropriate bin width, which could be used to distinguish different adjacent synchronized spikes from one another, 10-20 ms. These timing propagation profiles were then spike sorted as before by using the histogram shape as the spike. Results were examined manually and similar patterns were grouped together. A number of distinct propagation profiles within a given culture as well as the frequency of each kind of spike.

Jitter analysis

For jitter analysis, the electrode of interest served as the zero point of jitter for a most common spike, and jitter (standard deviation of timing, measured in μs) was calculated for all other electrodes in all other configurations.

Study II

MuSK+ EAMG model

MuSK+ EAMG was induced in 10 female C57BL6 wild type mice aged 8 weeks by active immunization of 10 μg of recombinant rat MuSK in complete Freund's adjuvant (CFA) subcutaneously. The control mice were immunized with CFA/PBS [123]. The inverted mesh hang-time test was used to measure of fatiguing weakness [9].

C2C12 muscle cell line

Immortalized C2C12 (ATCC® CRL- 1772™) mouse myoblast cell line was obtained from ATCC and cultured in growth medium consisting of Dulbecco's modified Eagle's medium (DMEM, Gibco™, 41966029) supplemented with 10% fetal bovine serum (Gibco™, 26140079), 1% Penicillin–Streptomycin (Gibco™, 15140122), at 37˚C and 8% CO_2.

Transfection of C2C12 cells with miRNA mimics

For transfection experiments following mirVana miRNA mimics (all from Ambion, Life Technologies) were used: mmu-miR-1933-3p (MC15467), mmu-miR-1930-5p (MC15244), mirVana™ miRNA mimic Negative Control

No.1 (Cat#: 4464058). C2C12 myoblasts were seeded into 12-well plate at density 7×10^4 cells/well and grown until approximately 70-80% confluency. At this point, cells were transfected with miRNA mimics at final concentration of 25nM using jetPrime® transfection reagent (Polyplus, Cat#: 114-15). The transfected cells were maintained in growth medium for 48 hours before harvesting for total RNA extraction.

MiRNA isolation and expression analysis in mouse muscles

MiRNA from the eight omohyoid muscles was isolated using the miRNeasy Mini Kit (Qiagen, cat. no. 217004), including enrichment of miRNAs with the RNeasy MinElute Cleanup Kit (Qiagen, cat. no. 74204), in accordance the manufacturer's instructions. Isolated RNA was used to synthesize cDNA using Universal cDNA Synthesis Kit II (Exiqon #203301, Vedbaek, Denmark) and the reaction was run in a T100™ Thermal Cycler (Bio-Rad). RT-qPCR was done on microRNA Ready-to-Use PCR Mouse & Rat Panel I+I (Exiqon), pre-coated with primers for 752 miRNAs. All miRNAs were assayed in duplicates. As quality controls, the interplate calibration (UniSp3) and cDNA synthesis control (UniSp6) were used. The cDNA reactions were diluted 200× in ExiLENT SYBR® Green master mix before being applied to the PCR panel plates. RT-qPCR was run for 40 amplification cycles on the Applied Biosystems 7900HT Fast Real-Time PCR System (Life Technologies). Relative miRNA expression was quantified using the ΔCT method [188].

mRNA expression analysis in transfected C2C12 cells

RNA quality, extracted from C2C12 cells, was evaluated using the Agilent 2100 Bioanalyzer system (Agilent Technologies Inc, Palo Alto, CA). Total RNA (250 ng) was used to generate amplified and biotinylated sense-strand cDNA from the entire expressed genome according to the GeneChip™ WT PLUS Reagent Kit manual Target Preparation for GeneChip™ Whole Transcript (WT) Expression Arrays User Guide (P/N 703174, ThermoFisher Scientific Inc., Life Technologies, Carlsbad, CA, USA) Clariom™ S Arrays (Clariom™ S Arrays, mouse) were hybridized for 16-18 hours in a 45°C incubator, rotated at 60 rpm. According to the GeneChip™ Expression Wash, Stain and Scan Manual (PN 702731, ThermoFisher Scientific Inc., Life Technologies, Carlsbad, CA, USA) the arrays were then washed and stained using the GeneChip™ Fluidics Station 450 and finally scanned using the GeneChip™ Scanner 3000 7G. For the purpose of RT-qPCR, cDNA was made using 1 µg of isolated RNA in a 20 µl reaction mix including 1 µl SuperScript III reverse transcriptase (Invitrogen), 1 µl of DTT (0.1M), 0.5 µl of RNAse inhibitor (RiboGrip RNAse inhibitor, Solis BioDyne) and the reaction was run in a T100™ Thermal Cycler (Bio-Rad) at 25°C for 5 min, 50°C for 60 min, 70°C for 15 min. Selected target mRNAs [BRCA1-interacting protein

1 (Brip1), mitochondrial ribosomal protein L27 (Mrpl27), myosin heavy chain 8 (Myh8), Inositol monophosphatase I (Impa1) and autophagy related protein 9b (Atg9b)] were assayed in duplicates. RT-qPCR reactions were carried out using the HOT FIREPol Eva Green qPCR Supermix (Solis BioDyne). Target amplification was performed using the 7900HT Fast Real-Time PCR System (Applied Biosystems). Relative miRNA expression was calculated using the ΔCT method [188].

To check the accumulation of the transfected miRNA mimics in C2C12 cells, total RNA was isolated with miRNeasy Mini Kit and cDNA was made using the Universal cDNA Synthesis Kit II as described above. The accumulation of the transfected miRNA mimics was analyzed with RT-qPCR using the ExiLENT SYBR® Green master mix and their expression was normalized to the SNORD68 RNA (Exiqon, cat#203911).

Western Blot analysis

Western blot analysis was performed to assess expression of Impa1 in cultured C2C12 myoblasts after transfection with miRNA mimics. Briefly, C2C12 cells seeded on 12-well culture plates were initially transfected with 25nM of mimics for 24 hours. Additional transfection with the same mimics was performed at a final concentration of 50nM for 48 hours. Cells were washed in PBS, lyzed in RIPA buffer and collected as lysates for analyzing by SDS-PAGE and western blotting as described previously[189]. Anti-Impa1 (Nordic Biosite, A305-428A-T), anti-actin (Santa Cruz, sc-1616) were used as a primary for western blotting. Protein expression was detected using the Odyssey scanner (LI-COR) and the protein signals were quantified using Image Studio Software (LI-COR)[189]

Statistical analysis

In order to obtain normally distributed data, the data were log-transformed. An unpaired two-tailed t-test was used to compare miRNA expression between the EAMG and control groups with a null hypothesis of equal means. Bonferroni-Holm method was applied for multiple comparison test. Statistical significance was defined as $p < 0.05$. The Exiqon GenEx software with unpaired t-test was used for comparison of miRNA levels between transfected groups. The raw data from the microarray analysis were normalized in the free software Expression Console, provided by Affymetrix (http://www.affymetrix.com), using the SST-RMA version of the robust multiarray average (RMA) method. The comparisons performed were miR1930-5p transfected cells versus negative controls and mir1933-3p transfected cells versus negative controls. Subsequent analysis of the gene expression data was carried out in the statistical computing language R (http://www.r-project.org) using packages available from the Bioconductor project (http://www.bioconductor.org).

In order to search for differentially expressed genes between the control and the treatment sample groups an empirical Bayes moderated t-test was applied, employing the 'limma' package (version 3.30.13). To address the problem with multiple testing, the p-values were adjusted using the method of Benjamini and Hochberg.

Study III

Primary myoblast culture

All experiments were approved by the Uppsala Animal Ethical Committee under animal license C97/15 and follow the guidelines of the Swedish Legislation on Animal Experimentation (Animal Welfare Act SFS 2009:303) and the European Communities Council Directive (2010/63/EU). A detailed protocol of the primary muscle cell culture growing on HD-MEA chips was described previously, in methods part for the Study I.

Application of neural agrin

Rat recombinant neuronal agrin (R & D systems, 550-AG-100) with a concentration of 100 pM was applied for 24 h on 4 and 10 days *in vitro* (DIV) on three HD-MEA chips, while the other three chips served as a control group. Daily recordings of the average spike amplitude were carried out up to 26 days of culture.

Immunostaining and microscopy

Cells were fixed and stain immediately after electrophysiological recordings. Briefly, after washing step with PBS, cells were fixed in 4% paraformaldehyde and permeabilized with 0.25% Triton X-100 in PBS. Unspecific binding was blocked by incubating cells in 1% BSA in PBS. Cells were then incubated with primary antibodies overnight at 4°C, washed, and then incubated with secondary antibodies for 1 h. Series of Z-stack images covering the entire electrode array was performed using a Carl Zeiss AxioImager or Nikon Eclipse LVDIA-N microscope. The images were stitched and analyzed with ImageJ plugins or Imaris 8.0 software.

The effect of recombinant rat agrin on clustering of AChRs

Primary myotubes were treated with 100 pM of recombinant rat agrin (R&D systems, 550-AG-100) on 20 DIV for 24h, and AChRs clusters were labeled in live cells by specific binding of fluorescently labeled α-Bungarotoxin, 2.5 μg/mL (Sigma-Aldrich, T0195). Additionally, anti-α-actinin (Abcam,

ab9465) was stained during immunostaining protocol. Images were acquired by using 60x oil objective and Nikon Eclipse LVDIA-N fluorescence microscope (Nikon). After deconvolution postprocess in Huygens software, the number and areas of AChR clusters were analyzed in Imaris software, where defined threshold parameters for individual AChR cluster were applied for all others images.

Correlation analysis between electrical activity and morphological features of skeletal myotube

The thickest parts of individual myotubes growing on HD-MEA chips were found after scrolling through the Z-stack, and the diameter was measured by drawing a perpendicular line relative to the direction of the myotube. The mean value of the myotube diameter was based on three individual measurements. The microphotography of the HD-MEA was integrated into Matlab and used to identify individual electrodes, match their location and registered electrical activity to the myotubes of interest.

Statistical analysis

Pearson's correlation analysis was used in order to find a correlation between the diameter of the myotubes and the individual spikes. Kolmogorov-Smirnov test was applied for the analysis of AChR cluster distribution between the myotubes treated with agrin and control groups. A p-value < 0.05 was considered significant.

Results and discussion

Paper I

We cultured primary myoblasts on HD-MEA chips for more than 60 days. The fusion of myoblasts into myotubes was seen on the second day after switching to differentiation medium. Within a few days (range from four to seven days), individual myotubes showed a spontaneous contraction, observed under the microscope. These contractions exhibited great variations of all gradations: from a rapid shallow tremble to a slow deep pulsation. Some myotubes contracted with constant frequency, while others followed a certain pattern: their contractions were interrupted by a sudden break with a rest period and further recovery of activity. The first electrical signals in the form of individual spikes we were able to record on HD-MEA chips near the end of the second week. In contrast, one of the few groups that used HD-MEA for the electrophysiological characterization of muscle cells, were able to measure such signals after three days of cultivation [190]. However, this early observation of electrical activity of cultured muscle is related to the intracellular recording performed by 3D-shaped microelectrode platform. Nevertheless, all our observations are consistent with previous studies about the maturation of muscle cells *in vitro*, where fully differentiated myotubes demonstrated well-organized cross-striations and also were undergo spontaneous contractions around 14 -20 DIV [191, 192].

It is equally important to explain the nature of spontaneous contractions in cultured myotubes in the absence of neuronal stimulation. The high frequency spontaneous electrical activity (> 1 Hz) in mouse myotubes may results from an interplay between Na^+, Ca^{2+} and Ca^{2+} - activated K^+ currents [193]. On the contrary, low frequency (<0.5 Hz) contraction can be induced by activation AChRs in response to the autocrine release of acetylcholine by myotubes [194]. Perhaps, simultaneous activity of different ion channels involved in spontaneous contraction can explain the large variety of spikes registered on HD-MEA chips (Figure 4). The observed spikes can differ in their amplitude, frequency, and shapes, which a range from short monophasic positive or monophasic negative spikes to long multiphasic spikes superimposed on each other. On the other hand, the simultaneous contraction of several cells located in close proximity to a given electrode can also lead to recording of overlapped extracellular currents in the shape of polymorphic spikes.

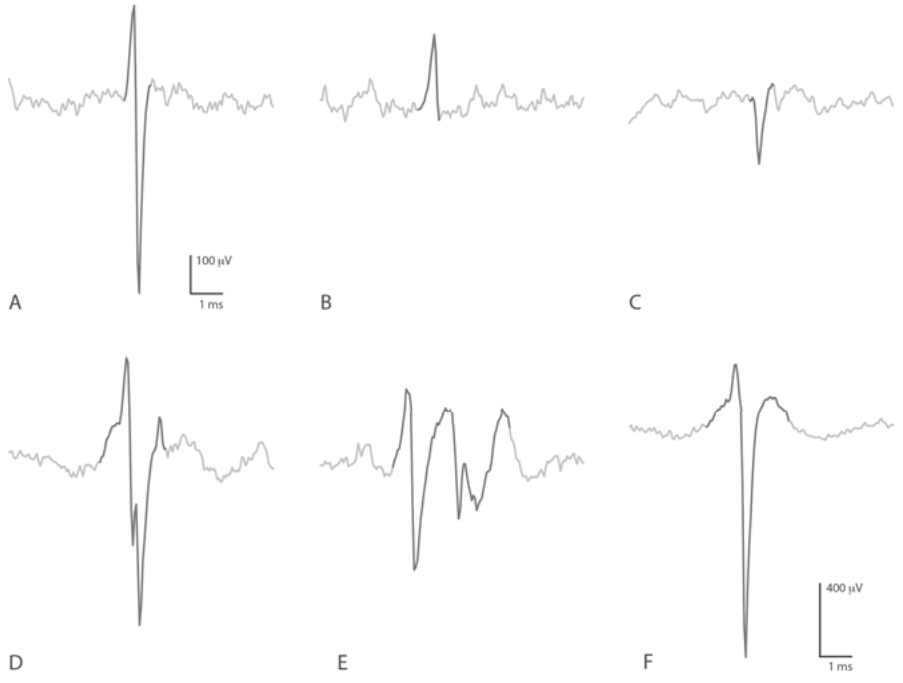

Figure 4. **Spontaneous spike shapes on different electrodes during a single recording session.** Biphasic spike (**A** and **F**) starting with a positive peak, was the most common shape observed during recordings. (**B** and **C**) Monophasic positive or negative spikes. The maturation of myotubes was accompanied by the appearance of more complicated multiphasic spikes (**D** and **E**).

Gradual complication in the variety of recorded signals also correlated with the dynamics of muscle culture. Initially, individual spikes were observed on a small number of electrodes, but over time this number increased. Further maturation of muscle cells was associated with appearance of small isolated islands of spikes, which slowly organized into much larger spiking areas. After about 20 days in culture, the assembled myotubes had effectively formed into a piece of muscle tissue that contracted at the same rate all across the chip.

At the same time, we observed individual areas with the highest spike amplitude, where the AP obviously appeared and spread to neighboring areas. We used jitter analysis to find the relationship between these neighboring areas and determine individual muscle units. Unlike healthy innervated muscles *in vivo*, where a jitter value of about 20-30 μs is considered normal, in our culture, we observed areas with jitter ≤ 50 μs, and with increasing distance from the selected electrode, jitter also increased to 100–150 μs. In clinical studies, an increased jitter value above 80–100 μs indicates impairment in neuromuscular transmission [195]. However, in our model, increased jitter values can be explained by the lack of innervation, which also complicates the detection of individual muscle units and their more detailed analysis.

One of the distinguishing advantages of the presented method is the ability to maintain an actively functioning muscle cell culture for a long period of time (more than 2 months). This feature is essential for studying neuromuscular diseases and normal physiology of muscle cells. The viability and development of the myotubes culture was assessed by several electrophysiological parameters. For instance, the number of electrodes capable to detect spikes gradually increased over time in a linear manner (Paper I, Figure 2A). The spikes amplitude and their frequency also progressively increased (Paper I, Figure 2B, 2C). Despite the obvious fluctuations reflecting the functional activity of myotubes, all observed parameters eventually reached a steady state.

Muscle cells often experience mechanical stress and demand a constant flow of nutrients and metabolites to restore their functionality. Perhaps the renovation process involves a certain state of rest, which can affect the spontaneous activity of the muscle culture.

In addition, the muscle cells by their origin require innervation by motor neurons. The absence of neuronal inputs during embryogenesis leads to degeneration [196], reduction in the numbers [197] and myotube size [198]. Furthermore, in the absence of innervation, expression of slow myosin heavy chain is disrupted [195], which affects the phenotype of muscle fibers. Therefore, the presence of a motor neuron component will determine the formation of functional NMJs and also contribute to the normal maturation of muscle fibers. Thus, co-culture muscle cells with motor neurons would represent a more physiologically relevant model of the healthy and diseased NMJ that can be used as a platform to assess pharmaceutical treatments.

Paper II

This study focused on the dysregulation of intracellular miRNAs in skeletal muscles of the bulbar area, particularly the omohyoid muscle of mice with MuSK+ EAMG. The omohyoid muscle is clinically involved in the dysphagia associated with MuSK+ EAMG and MuSK+ MG [199], and was shown to develop severe pre- and postsynaptic disassembly as a result of the MuSK attack [123, 200]. A screening of 752 miRNAs was performed on RNA isolated from omohyoid muscles of four MuSK+ EAMG mice, two with moderate weakness and two with severe weakness, and four healthy control mice. We found that 15 miRNAs were significantly increased and three miRNAs were significantly decreased in muscles of mice with MuSK+ EAMG compared to controls (Paper II, Table 1 and Figure 1). Two of the most elevated miRNAs in atrophic muscles of MuSK+ EAMG mice were miR-1933-3p and miR-1930-5p, and therefore we proposed the hypothesis that these specific miRNAs can act on the processes involved in the regulation of important skeletal muscle proteins. Data analysis of mRNA expression level in the C2C12 cell line transfected with mimics of these miRNAs revealed the significant

downregulation of expression level for 21 mRNA transfected with miR-1933-3p and 7 mRNA transfected with miR-1930-5p (Paper II, Tables 2A and 2B).

Programs that predict binding sites for miRNAs showed that 5 of the detected mRNAs contain binding sites for miR-1933-3p: BRCA1-interacting protein 1 (Brip1), mitochondrial ribosomal protein L27 (Mrpl27), myosin heavy chain 8 (Myh8), Inositol polyphosphate-5-phosphatase A (Inpp5a) and Inositol monophosphate I (Impa1). Also, stannin (Snn) mRNA, a mitochondrial membrane protein, contained binding sites for miR-1930-3p. Interestingly, one mRNA of Atg9b, which was downregulated in by both mimics did not have predicted miRNA binding sites in all the programs.

Further analysis by RT-qPCR demonstrated significant reduction of the mRNA expression level of Mrpl27 ($p=0.04$) and Impa1 ($p=0.02$) in miR-1933-3p transfected C2C12 cells compared to control mimic transfected cells. Others potential targets mRNAs did not change significantly or had a very low expression level in C2C12 cells.

According to several databases (www.proteinatlas.org; www.genecards.org) Impa1 is well-expressed in skeletal muscles; however, there is no evidence supporting its involvement in any muscle disease. This gene encodes an enzyme that dephosphorylates myo-inositol monophosphate to generate free myo-inositol, a precursor of phosphatidylinositol, and is therefore an important modulator of intracellular signal transduction via the production of the second messengers myoinositol 1,4,5-trisphosphate and diacylglycerol [201]. This enzyme is inhibited by therapeutic concentrations of lithium to treat bipolar disorder [202]. It is known that patients with MG develop skeletal muscle fatigue and weakness after treatment with lithium [203]. Therefore, a decrease in the expression of Impa1 protein due to an increase in miR-1933-3p level can also lead to similar impairments.

Another interesting target for miR-1933-3p is Mrpl27, which is involved in mitochondrial translation and organelle biogenesis and maintenance. One previous report indicated mitochondrial dysfunction in muscles obtained from MuSK+ EAMG mice, through increased amount of red ragged fibers and significantly reduced citrate synthase SDH and NADH-cytochrome c-reductase enzyme activity [204]. Therefore, we propose that Mrpl27 could be the candidate target, and a direct link, to the previously observed mitochondrial dysfunction and muscle atrophy in MuSK+ EAMG [204].

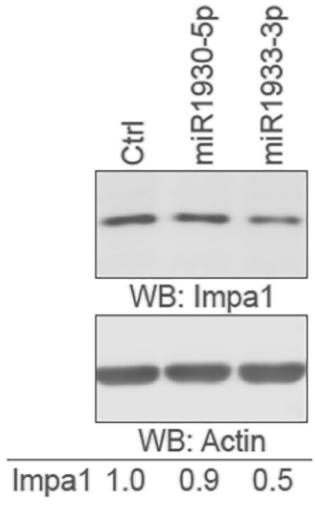

Figure 5. **Expression of the Impa1 protein.** C2C12 cells transfected with control (Ctrl; n=3), miR-1930-5p (n=3) and miR-1933-3p (n=3) mimics were analyzed for the Impa1 protein accumulation. The Impa1 protein levels were normalized to the actin protein (Impa1/actin) and relative expression is shown below the western blot images.

Additionally, we wanted to confirm the mRNA data on the protein level through western blot. Normalization to actin revealed that protein levels of Impa1 was reduced by 50% in the C2C12 cells transfected with miR-1933-3p, whereas Impa1 levels were comparable between control cells and those transfected with miR-1930-5p (Figure 5).

In conclusion, these data provide a new insight into dysregulated miRNAs and their intracellular pathways in muscle tissue affected by MuSK + EAMG.

Paper III

In this study, we sought to find the correlation between the morphological structures of skeletal muscles and their electrical activity as it was predicted in simulation studies on skeletal muscles *in vivo*. These studies demonstrated a direct correlation between the amplitude of the muscle AP and the diameter of the muscle fiber [205]. Our previous results show that myotubes growing on HD-MEA chips form a single muscle tissue after approximately three weeks of culture, which complicates a more detailed analysis of their electrical activity. Therefore, experiments in this study were performed at earlier developmental stages (10 DIV) when myotubes already expresses contractile proteins, like alpha-actinin and demonstrate nonsynchronous electrical activity. The mean value of thickness of individual muscle fibers (n = 179) was 11.04

± 3.53 µm, whereas the mean value for the myotubes growing in close contact to each other (n = 65) was 16.63 ± 3.65 µm. The general maximum thickness of myotubes was approximately 25 µm and the minimum thickness was approximately 4 µm. Data analysis of the electrical activity recorded in areas with individual muscle fibers, and in areas with a dense appearance of muscle fibers didn't reveal any correlation between the thickness and most negative amplitudes obtained on electrodes of interest in both groups (Fig 6a: r^2=0.01012; p=0.1803 and 6b: r^2=0.0235; p=0.5510).

The most likely explanation for the lack of a direct correlation between the thickness of the myotubes and the spike amplitude is the absence of a neuronal component in our model and that all measurements were performed at a relatively early stage of development. At the same time, an *in vivo* studies in mice showed a heterogeneous relationship between muscle fiber diameter and NMJ morphology [206].

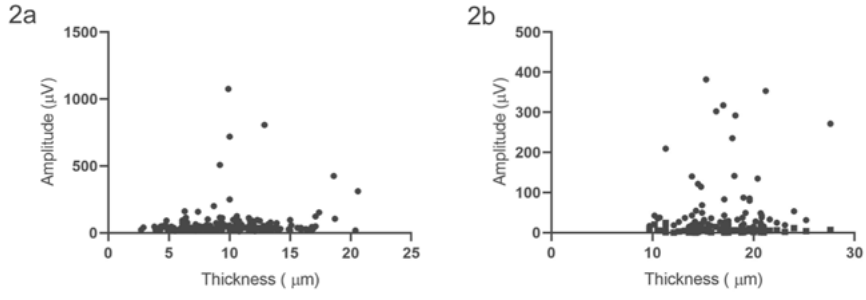

Figure 6. **Amplitude of the muscle AP plotted against thickness of the muscle fiber over that particular electrode.**

Formation of AChR clusters as well as other processes involved in postsynaptic differentiation of NMJ are controlled by factors released from axon terminal of motor neurons. However, AChRs already expressed at an early stage of skeletal muscle development promoting the fusion of myoblasts into myotubes [207, 208] and form embryonic clusters due to autoactivation of MuSK, regardless of innervation by motor neurons [13, 209]. Treatment with alpha-bungarotoxin inhibits spontaneous activity in the early stages of myogenesis and confirm involvement of AChRs at this process. Moreover, the synthesis and release of an endogenous cholinergic agonist by the myotubes themselves may underlie the mechanism of autocrine activation of AChRs in the absence of neuronal stimulation [210]. Taking advantage of our model system to grow primary myotubes for more than 20 days, we tried to evaluate the contribution of AChRs to the spontaneous electrical activity in the late stages of development. We decided to compensate the absence of neuronal component in our system by adding recombinant neuronal agrin, which stabilizes AChR to levels characteristic of innervated NMJs [211].

Data analysis indicated a great variety of AChRs and their clusters in both groups: from individual small dots uniting into small-sized groups, to elongated, narrow clusters, and rare formations resembling plaque-like clusters similar to the shape of an innervated NMJ *in vivo* (Paper III, Figure 3). In the control group, the median AChR size was 2.1 μm^2 (CI: 1.0-4.1; min. 0.49 and max. 110.5 μm^2), and in the agrin-treated group, the median size was 1.9 μm^2 (CI: 1.0-4.2; min. 0.002 and max. 97.7 μm^2) ($p < 0.0001$). The number of AChR clusters with an area of <1 μm^2 was 471 (20%) in the control group and 894 (25%) in the agrin-treated group. The largest number of clusters in a percentage ratio was observed in the size range of 1-5 μm^2 and was 1415 clusters (60%) in the control group and 1903 clusters (54%) in the agrin-treated group (Figure 7-II). These data indicate a significantly larger number of AChRs and AChR clusters in myotubes treated with neural agrin. At the same time, the *in vivo* studies depict an AChR cluster area in the calf muscle the diaphragm[212], which is significantly higher than most cluster sizes observed in our data.

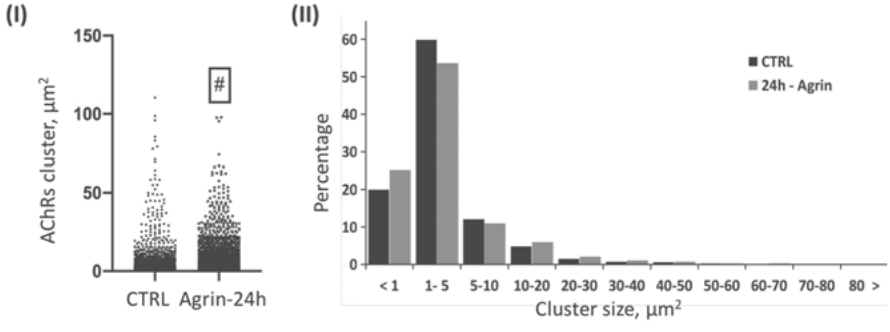

Figure 7. Quantification analysis of AChR cluster formation in control group (N=2364) and treated with recombinant rat agrin (N=3548) (I) Quantification of AChR cluster area size. P<0.0001, CTRL vs. Agrin-24h, Kolmogorov-Smirnov test. (II) Percentage distribution of different cluster sizes.

In order to identify a possible effect of neural agrin on spontaneous electrical activity of myotubes, we performed daily recordings for a total of 26 days. Three chips were treated with recombinant rat agrin at 4 and 10 DIV, while others three chips were maintained under standard conditions and used as a control group. Already on the 4th day of culturing myotubes in differentiation medium, we observed activity on individual electrodes in both groups. However, the number of electrodes recording electric activity in the agrin-treated group increased by 6 DIV compared to the control group, and in some parts of the activity maps, electrode alignment was observed in parallel lines (12 DIV), which suggests the development of elongated myotube forms. We also applied 100 nM ACh to the extracellular solution at 20 DIV to stimulate the activity of AChRs, but did not observe any difference in electrical activity

before and after treatment (data not shown). Unfortunately, one of the chips belonging to the agrin-processed group was unable to connect to the recording device due to a technical malfunction of the chip and was therefore excluded from the experiments. At the same time, most of the myotubes cultured on another HD-MEA chip with agrin-treated myotubes detached from the surface of the chip on day 22, most likely due to intense contractions, and only a small fraction continued to show high activity on the right the angle of this chip (Paper III, Figure 5). However, myotubes cultured on control chips also began to show increased activity on the entire array of electrodes at a later stage of development (24 DIV).

In conclusion, our results indicate the possible involvement of neural agrin in the spontaneous electrical activity generated by muscle cells in the early stages of development. However, we did not observe any functional effects of agrin at a later stage of development.

Future studies

In the future, we are planning to establish the complete NMJ on the HD-MEA chip. This NMJ modelling will be completed by co-culturing motor neurons and muscle cells on the chip. Owing to thousands of densely packed microelectrodes, these arrays offer the potential to access electrical activity of the NMJ at subcellular spatial resolution and, as such, can be used to investigate functional interplay between pre- and postsynaptic elements during the process of formation and disruption of the NMJ. Physical separation of cells through the application of microfluidic systems also should help to mimic more closely the physiological conditions. Furthermore, this type of engineered constructs provides easier and more direct manipulations to the cell culture, such as administration of antibodies or miRNAs in order to better understand their role in development of neuromuscular degenerative disorders.

Along with the application of well-established animal cell models of animal origin and cell lines, the introduction of human pluripotent stem cells (hPSCs) for tissue engineering and complex disease modeling is also expanding. A major advantage of using hPSCs for muscle bioengineering is the ability to derive different cell types from the same cellular source and to study molecular pathways involved in NMJ dysfunction. The generation of functional hPSC-derived NMJ models will provide the possibility for the discovery of drug treatments that may improve neuromuscular function and restore muscle contractility in patients. We also plan to establish hPSC-derived NMJ model for detail electrophysiological characterization on HD-MEA chips.

As shown by our own and other recent studies, miRNAs can serve not only as biomarkers indicating the presence of a disease, but also can actively influence the course of its development. Therefore, we plan to study the effects of disease specific miRNA on cells on the chip (motor neurons and muscle cells).

Conclusions

In conclusion, our main findings were the following:

- We were successful in establishing a long-term muscle cell culture on HD-MEA chips, allowing for tracking of the development extracellular features of muscle cells.
- The myotube maturation and fusion into mature muscle tissue was accompanied by a gradual increase in the amplitude and frequency of individual electrical spikes.
- The contraction activity of mature muscle tissue had common spiking frequency across the chip, with individual spikes arising in different parts of the culture and propagating in opposite directions at various speeds.
- The observed electrical activity of mature muscle fibers is well correlated with images obtained using fluorescence microscope.
- Findings of novel miRNAs that are dysregulated in muscle tissue afflicted with MuSK+ EAMG, provide insight into the effects of this disease on the posttranscriptional level.
- There is no direct correlation between the amplitudes of MAPs and the diameter of myotubes in their early developmental stage.
- Agrin application seems to enhance the development of aneural myotubes in increasing the number of AChR clusters and promoting spontaneous activity at an early developmental stage.

Acknowledgments

I am sincerely grateful to all those people who contributed to this work, providing me incredible support, helping, educating and inspiring me.

Firstly, I would like to thank my supervisor **Anna Rostedt Punga** for having confidence in me and giving me the opportunity to become a PhD student in your group. I am grateful for your endless optimism and for your kind support during these four years. I also very much appreciate your constructive criticism, comments, and proofreading of my thesis. Thank you so much!

I am very grateful to **Tanel Punga** for introducing me to the world of molecular biology and microRNA. Your outstanding knowledge and great support helped to overcome some of the setbacks and successfully complete the second project.

Thank you very much! I also express my special thanks to my co-supervisor **Klas Kullander** for his timely and valuable advice regarding my research path and further steps towards the PhD.

I would also like to warmly thank all the past and present members of the Clinical Neurophysiology group:

I was fortunate enough to start working with **Marta Lewandowska** at the beginning of my PhD. I will always gratefully recall the time when we could find a reason for a loud laugh between our experiments. Marta, thanks for all the positive motivations, moral support, and an open mind. I would like to thank **Milos Radivojevic** for sharing his extensive laboratory experience, helpful criticism and showing remarkable patience while explaining to me the theoretical principles of sorting electrical signals. I am grateful to **Liis Sabre** for teaching me how to deal with PCR robot and for an excellent lab journal where I could easily find comprehensive information for my experiments. **Carl Johan Molin**, thanks for giving me a great example of highly organized work and self-discipline. **Markus de Ruijter**, I will miss your delicious cakes, and thank you and **Yu-Fang Huang** for the beautiful flower on my shelf that you planted for me and continue to care for. Special thanks to the undergraduate students of our lab, **Emma Wallberg**, **Elina Svensson**, **Monika Budrytė** and **Anna Popova**, for giving me the opportunity to also be in the role of a "boss". I very appreciate all your research assistance in our group. Thank you!

Finally, I am also very grateful to **Dirk Pacholsky**, **Matyas Molnar** and **Jeremy Adler** from the BioVis platform of Uppsala University. Your friendly and competent support helped me to get beautiful images of my work.

References

1. Li, L., W.C. Xiong, and L. Mei, *Neuromuscular Junction Formation, Aging, and Disorders.* Annu Rev Physiol, 2018. **80**: p. 159-188.
2. Tintignac, L.A., H.R. Brenner, and M.A. Ruegg, *Mechanisms Regulating Neuromuscular Junction Development and Function and Causes of Muscle Wasting.* Physiol Rev, 2015. **95**(3): p. 809-52.
3. Punga, A.R. and M.A. Ruegg, *Signaling and aging at the neuromuscular synapse: lessons learnt from neuromuscular diseases.* Curr Opin Pharmacol, 2012. **12**(3): p. 340-6.
4. Engel, A.G., *Genetic basis and phenotypic features of congenital myasthenic syndromes.* Handb Clin Neurol, 2018. **148**: p. 565-589.
5. McMacken, G., et al., *The Increasing Genetic and Phenotypical Diversity of Congenital Myasthenic Syndromes.* Neuropediatrics, 2017. **48**(4): p. 294-308.
6. Gilhus, N.E., et al., *Myasthenia gravis - autoantibody characteristics and their implications for therapy.* Nat Rev Neurol, 2016. **12**(5): p. 259-68.
7. Viegas, S., et al., *Passive and active immunization models of MuSK-Ab positive myasthenia: electrophysiological evidence for pre and postsynaptic defects.* Exp Neurol, 2012. **234**(2): p. 506-12.
8. Straasheijm, K.R., et al., *Muscle-specific kinase myasthenia gravis IgG4 autoantibodies cause severe neuromuscular junction dysfunction in mice.* Brain, 2012. **135**(4): p. 1081-1101.
9. Phillips, W.D., et al., *Guidelines for pre-clinical animal and cellular models of MuSK-myasthenia gravis.* Exp Neurol, 2015. **270**: p. 29-40.
10. Dawson, T.M., T.E. Golde, and C. Lagier-Tourenne, *Animal models of neurodegenerative diseases.* Nature Neuroscience, 2018. **21**(10): p. 1370-1379.
11. Slater, C.R., *The Structure of Human Neuromuscular Junctions: Some Unanswered Molecular Questions.* Int J Mol Sci, 2017. **18**(10).
12. Nicholls, J.G., *How acetylcholine gives rise to current at the motor end-plate.* J Physiol, 2007. **578**(Pt 3): p. 621-2.
13. Lin, W., et al., *Distinct roles of nerve and muscle in postsynaptic differentiation of the neuromuscular synapse.* Nature, 2001. **410**(6832): p. 1057-64.
14. Yang, X., et al., *Patterning of muscle acetylcholine receptor gene expression in the absence of motor innervation.* Neuron, 2001. **30**(2): p. 399-410.
15. Campanelli, J.T., et al., *Agrin mediates cell contact-induced acetylcholine receptor clustering.* Cell, 1991. **67**(5): p. 909-16.
16. Ruegg, M.A., et al., *The agrin gene codes for a family of basal lamina proteins that differ in function and distribution.* Neuron, 1992. **8**(4): p. 691-9.
17. DeChiara, T.M., et al., *The receptor tyrosine kinase MuSK is required for neuromuscular junction formation in vivo.* Cell, 1996. **85**(4): p. 501-12.
18. Kim, N., et al., *Lrp4 is a receptor for Agrin and forms a complex with MuSK.* Cell, 2008. **135**(2): p. 334-42.

19. Zhang, B., et al., *LRP4 serves as a coreceptor of agrin.* Neuron, 2008. **60**(2): p. 285-97.
20. Gomez, A.M. and S.J. Burden, *The extracellular region of Lrp4 is sufficient to mediate neuromuscular synapse formation.* Dev Dyn, 2011. **240**(12): p. 2626-33.
21. Zhang, W., et al., *Agrin binds to the N-terminal region of Lrp4 protein and stimulates association between Lrp4 and the first immunoglobulin-like domain in muscle-specific kinase (MuSK).* J Biol Chem, 2011. **286**(47): p. 40624-30.
22. Inoue, A., et al., *Dok-7 activates the muscle receptor kinase MuSK and shapes synapse formation.* Sci Signal, 2009. **2**(59): p. ra7.
23. Okada, K., et al., *The muscle protein Dok-7 is essential for neuromuscular synaptogenesis.* Science, 2006. **312**(5781): p. 1802-5.
24. Burden, S.J., R.L. DePalma, and G.S. Gottesman, *Crosslinking of proteins in acetylcholine receptor-rich membranes: association between the beta-subunit and the 43 kd subsynaptic protein.* Cell, 1983. **35**(3 Pt 2): p. 687-92.
25. Gautam, M., et al., *Failure of postsynaptic specialization to develop at neuromuscular junctions of rapsyn-deficient mice.* Nature, 1995. **377**(6546): p. 232-6.
26. Ramarao, M.K. and J.B. Cohen, *Mechanism of nicotinic acetylcholine receptor cluster formation by rapsyn.* Proc Natl Acad Sci U S A, 1998. **95**(7): p. 4007-12.
27. Sealock, R., B.E. Wray, and S.C. Froehner, *Ultrastructural localization of the Mr 43,000 protein and the acetylcholine receptor in Torpedo postsynaptic membranes using monoclonal antibodies.* J Cell Biol, 1984. **98**(6): p. 2239-44.
28. Marchand, S., et al., *Rapsyn escorts the nicotinic acetylcholine receptor along the exocytic pathway via association with lipid rafts.* J Neurosci, 2002. **22**(20): p. 8891-901.
29. Moransard, M., et al., *Agrin regulates rapsyn interaction with surface acetylcholine receptors, and this underlies cytoskeletal anchoring and clustering.* J Biol Chem, 2003. **278**(9): p. 7350-9.
30. Zuber, B. and N. Unwin, *Structure and superorganization of acetylcholine receptor-rapsyn complexes.* Proc Natl Acad Sci U S A, 2013. **110**(26): p. 10622-7.
31. Bartoli, M., M.K. Ramarao, and J.B. Cohen, *Interactions of the rapsyn RING-H2 domain with dystroglycan.* J Biol Chem, 2001. **276**(27): p. 24911-7.
32. Dobbins, G.C., et al., *alpha-Actinin interacts with rapsyn in agrin-stimulated AChR clustering.* Mol Brain, 2008. **1**: p. 18.
33. Zhang, B., et al., *Beta-catenin regulates acetylcholine receptor clustering in muscle cells through interaction with rapsyn.* J Neurosci, 2007. **27**(15): p. 3968-73.
34. van Amerongen, R. and R. Nusse, *Towards an integrated view of Wnt signaling in development.* Development, 2009. **136**(19): p. 3205-3214.
35. Messeant, J., et al., *Wnt proteins contribute to neuromuscular junction formation through distinct signaling pathways.* Development, 2017. **144**(9): p. 1712-1724.
36. Nusse, R., et al., *A new nomenclature for int-1 and related genes: the Wnt gene family*. Cell, 1991. **64**(2): p. 231.
37. Behrens, J., *Everything you would like to know about wnt signaling.* Sci. Signal., 2013. **6**(275): p. pe17-pe17.
38. Gordon, M.D. and R. Nusse, *Wnt signaling: multiple pathways, multiple receptors, and multiple transcription factors.* J Biol Chem, 2006. **281**(32): p. 22429-33.

39. Niehrs, C., *The complex world of WNT receptor signalling.* Nature reviews Molecular cell biology, 2012. **13**(12): p. 767.
40. Hubbard, S.R. and K. Gnanasambandan, *Structure and activation of MuSK, a receptor tyrosine kinase central to neuromuscular junction formation.* Biochimica et Biophysica Acta (BBA)-Proteins and Proteomics, 2013. **1834**(10): p. 2166-2169.
41. Luo, Z.G., et al., *Regulation of AChR clustering by Dishevelled interacting with MuSK and PAK1.* Neuron, 2002. **35**(3): p. 489-505.
42. Messeant, J., et al., *MuSK frizzled-like domain is critical for mammalian neuromuscular junction formation and maintenance.* J Neurosci, 2015. **35**(12): p. 4926-41.
43. Strochlic, L., et al., *Wnt4 participates in the formation of vertebrate neuromuscular junction.* PLoS One, 2012. **7**(1): p. e29976.
44. Barik, A., et al., *Crosstalk between Agrin and Wnt signaling pathways in development of vertebrate neuromuscular junction.* Developmental neurobiology, 2014. **74**(8): p. 828-838.
45. Henriquez, J.P., et al., *Wnt signaling promotes AChR aggregation at the neuromuscular synapse in collaboration with agrin.* Proceedings of the National Academy of Sciences, 2008. **105**(48): p. 18812-18817.
46. Zhang, B., et al., *Wnt proteins regulate acetylcholine receptor clustering in muscle cells.* Molecular brain, 2012. **5**(1): p. 7.
47. Wang, J., et al., *Wnt/β-catenin signaling suppresses Rapsyn expression and inhibits acetylcholine receptor clustering at the neuromuscular junction.* Journal of Biological Chemistry, 2008. **283**(31): p. 21668-21675.
48. Li, X.-M., et al., *Retrograde regulation of motoneuron differentiation by muscle β-catenin.* Nature neuroscience, 2008. **11**(3): p. 262.
49. Liu, Y., et al., *β-Catenin stabilization in skeletal muscles, but not in motor neurons, leads to aberrant motor innervation of the muscle during neuromuscular development in mice.* Developmental biology, 2012. **366**(2): p. 255-267.
50. Wu, H., et al., *β-Catenin gain of function in muscles impairs neuromuscular junction formation.* Development, 2012. **139**(13): p. 2392-2404.
51. Frontera, W.R. and J. Ochala, *Skeletal muscle: a brief review of structure and function.* Calcif Tissue Int, 2015. **96**(3): p. 183-95.
52. Feher, J., *3.4 - Skeletal Muscle Mechanics*, in *Quantitative Human Physiology (Second Edition)*, J. Feher, Editor. 2017, Academic Press: Boston. p. 292-304.
53. Schiaffino, S. and C. Reggiani, *Fiber Types in Mammalian Skeletal Muscles.* Physiological Reviews, 2011. **91**(4): p. 1447-1531.
54. Silverthorn, D.U., et al., *Human physiology : an integrated approach*. 2016.
55. Hesse, B., M.S. Fischer, and N. Schilling, *Distribution pattern of muscle fiber types in the perivertebral musculature of two different sized species of mice.* Anat Rec (Hoboken), 2010. **293**(3): p. 446-63.
56. Biolo, G., et al., *Increased rates of muscle protein turnover and amino acid transport after resistance exercise in humans.* Am J Physiol, 1995. **268**(3 Pt 1): p. E514-20.
57. Fry, A.C., *The role of resistance exercise intensity on muscle fibre adaptations.* Sports Med, 2004. **34**(10): p. 663-79.
58. MacDougall, J.D., et al., *Changes in muscle protein synthesis following heavy resistance exercise in humans: a pilot study.* Acta Physiol Scand, 1992. **146**(3): p. 403-4.
59. Argiles, J.M., et al., *Muscle wasting in cancer and ageing: cachexia versus sarcopenia.* Adv Gerontol, 2006. **18**: p. 39-54.

60. Wall, B.T., M.L. Dirks, and L.J. van Loon, *Skeletal muscle atrophy during short-term disuse: implications for age-related sarcopenia.* Ageing Res Rev, 2013. **12**(4): p. 898-906.
61. Krauss, R.S., G.A. Joseph, and A.J. Goel, *Keep Your Friends Close: Cell-Cell Contact and Skeletal Myogenesis.* Cold Spring Harb Perspect Biol, 2017. **9**(2).
62. Cossu, G. and S. Biressi, *Satellite cells, myoblasts and other occasional myogenic progenitors: possible origin, phenotypic features and role in muscle regeneration.* Semin Cell Dev Biol, 2005. **16**(4-5): p. 623-31.
63. Comai, G. and S. Tajbakhsh, *Molecular and cellular regulation of skeletal myogenesis.* Curr Top Dev Biol, 2014. **110**: p. 1-73.
64. Cech, D.J. and S.T. Martin, *Chapter 7 - Muscle System Changes*, in *Functional Movement Development Across the Life Span (Third Edition)*, D.J. Cech and S.T. Martin, Editors. 2012, W.B. Saunders: Saint Louis. p. 129-150.
65. Blake, J.A. and M.R. Ziman, *Pax genes: regulators of lineage specification and progenitor cell maintenance.* Development, 2014. **141**(4): p. 737-51.
66. Punch, V.G., A.E. Jones, and M.A. Rudnicki, *Transcriptional networks that regulate muscle stem cell function.* Wiley Interdiscip Rev Syst Biol Med, 2009. **1**(1): p. 128-140.
67. Braun, T. and M. Gautel, *Transcriptional mechanisms regulating skeletal muscle differentiation, growth and homeostasis.* Nat Rev Mol Cell Biol, 2011. **12**(6): p. 349-61.
68. Rudnicki, M.A., et al., *MyoD or Myf-5 is required for the formation of skeletal muscle.* Cell, 1993. **75**(7): p. 1351-9.
69. Faralli, H. and F.J. Dilworth, *Turning on myogenin in muscle: a paradigm for understanding mechanisms of tissue-specific gene expression.* Comp Funct Genomics, 2012. **2012**: p. 836374.
70. Kassar-Duchossoy, L., et al., *Mrf4 determines skeletal muscle identity in Myf5:Myod double-mutant mice.* Nature, 2004. **431**(7007): p. 466-71.
71. Charge, S.B. and M.A. Rudnicki, *Cellular and molecular regulation of muscle regeneration.* Physiol Rev, 2004. **84**(1): p. 209-38.
72. Mauro, A., *SATELLITE CELL OF SKELETAL MUSCLE FIBERS.* The Journal of Biophysical and Biochemical Cytology, 1961. **9**(2): p. 493-495.
73. Seale, P., et al., *Pax7 is required for the specification of myogenic satellite cells.* Cell, 2000. **102**(6): p. 777-86.
74. Wang, Y.X. and M.A. Rudnicki, *Satellite cells, the engines of muscle repair.* Nat Rev Mol Cell Biol, 2011. **13**(2): p. 127-33.
75. Le Grand, F. and M.A. Rudnicki, *Skeletal muscle satellite cells and adult myogenesis.* Curr Opin Cell Biol, 2007. **19**(6): p. 628-33.
76. Barrett, K.E., et al., *Excitable Tissue: Muscle*, in *Ganong's Review of Medical Physiology, 25e*. 2016, McGraw-Hill Education: New York, NY.
77. Feher, J., *3.5 - Contractile Mechanisms in Skeletal Muscle*, in *Quantitative Human Physiology (Second Edition)*. 2017, Academic Press: Boston. p. 305-317.
78. Hall, J.E., *Guyton and Hall textbook of medical physiology*. 2016.
79. von der Ecken, J., et al., *Structure of the F-actin-tropomyosin complex.* Nature, 2015. **519**(7541): p. 114-7.
80. Wegner, A., *Equilibrium of the actin-tropomyosin interaction.* J Mol Biol, 1979. **131**(4): p. 839-53.
81. Rhoades, R. and D.R. Bell, *Medical Physiology, International Edition: Principles for Clinical Medicine*. 2017: Lippincott Williams&Wilki.

82. Knowles, A.C., M. Irving, and Y.B. Sun, *Conformation of the troponin core complex in the thin filaments of skeletal muscle during relaxation and active contraction.* J Mol Biol, 2012. **421**(1): p. 125-37.
83. Craig, R. and W. Lehman, *Crossbridge and tropomyosin positions observed in native, interacting thick and thin filaments.* J Mol Biol, 2001. **311**(5): p. 1027-36.
84. McKillop, D.F. and M.A. Geeves, *Regulation of the interaction between actin and myosin subfragment 1: evidence for three states of the thin filament.* Biophys J, 1993. **65**(2): p. 693-701.
85. Lehman, W., et al., *Tropomyosin and actin isoforms modulate the localization of tropomyosin strands on actin filaments.* J Mol Biol, 2000. **302**(3): p. 593-606.
86. Chandy, I.K., J.C. Lo, and R.D. Ludescher, *Differential mobility of skeletal and cardiac tropomyosin on the surface of F-actin.* Biochemistry, 1999. **38**(29): p. 9286-94.
87. Henderson, C.A., et al., *Overview of the Muscle Cytoskeleton.* Compr Physiol, 2017. **7**(3): p. 891-944.
88. Ottenheijm, C.A. and H. Granzier, *Lifting the nebula: novel insights into skeletal muscle contractility.* Physiology (Bethesda), 2010. **25**(5): p. 304-10.
89. Fill, M. and J.A. Copello, *Ryanodine receptor calcium release channels.* Physiol Rev, 2002. **82**(4): p. 893-922.
90. Feher, J., *3.6 - The Neuromuscular Junction and Excitation–Contraction Coupling*, in *Quantitative Human Physiology (Second Edition)*. 2017, Academic Press: Boston. p. 318-333.
91. Feher, J., *3.2 - The Action Potential*, in *Quantitative Human Physiology (Second Edition)*. 2017, Academic Press: Boston. p. 265-279.
92. Duman, J.G. and J.G. Forte, *What is the role of SNARE proteins in membrane fusion?* Am J Physiol Cell Physiol, 2003. **285**(2): p. C237-49.
93. Jurkat-Rott, K., M. Fauler, and F. Lehmann-Horn, *Ion channels and ion transporters of the transverse tubular system of skeletal muscle.* Journal of Muscle Research & Cell Motility, 2006. **27**(5): p. 275-290.
94. Lee, E.H., *Ca2+ channels and skeletal muscle diseases.* Prog Biophys Mol Biol, 2010. **103**(1): p. 35-43.
95. Shamoo, A.E. and D.H. MacLennan, *A Ca++-dependent and -selective ionophore as part of the Ca++ plus Mg++-dependent adenosinetriphosphatase of sarcoplasmic reticulum.* Proc Natl Acad Sci U S A, 1974. **71**(9): p. 3522-6.
96. Hodgkin, A. and P. Horowicz, *The influence of potassium and chloride ions on the membrane potential of single muscle fibres.* The Journal of physiology, 1959. **148**(1): p. 127-160.
97. Adrian, R., W. Chandler, and A. Hodgkin, *Voltage clamp experiments in striated muscle fibres.* The Journal of physiology, 1970. **208**(3): p. 607-644.
98. Allard, B. and O. Rougier, *Reappraisal of the role of sodium ions in excitation-contraction coupling in frog twitch muscle.* Journal of Muscle Research & Cell Motility, 1992. **13**(1): p. 117-125.
99. DiFranco, M., A. Herrera, and J.L. Vergara, *Chloride currents from the transverse tubular system in adult mammalian skeletal muscle fibers.* The Journal of general physiology, 2011. **137**(1): p. 21-41.
100. Lefebvre, R., et al., *Whole-cell voltage clamp on skeletal muscle fibers with the silicone-clamp technique*, in *Patch-Clamp Methods and Protocols*. 2014, Springer. p. 159-170.

101. Ursu, D., R. Schuhmeier, and W. Melzer, *Voltage-controlled Ca2+ release and entry flux in isolated adult muscle fibres of the mouse.* The Journal of physiology, 2005. **562**(2): p. 347-365.
102. Lehmann-Horn, F., et al., *Principles of Electrophysiological In Vitro Measurements*, in *Cardiac Electrophysiology Methods and Models*, D.C. Sigg, et al., Editors. 2010, Springer US: Boston, MA. p. 119-134.
103. Neher, E. and B. Sakmann, *Single-channel currents recorded from membrane of denervated frog muscle fibres.* Nature, 1976. **260**(5554): p. 799.
104. Basmajian, J.V. and C.J. De Luca, *Muscles alive: their functions revealed by electromyography*. Vol. 5. 1985: Williams & Wilkins Baltimore.
105. Mendelson, Y., *Chapter 10 - Biomedical Sensors*, in *Introduction to Biomedical Engineering (Third Edition)*, J.D. Enderle and J.D. Bronzino, Editors. 2012, Academic Press: Boston. p. 609-666.
106. Aminoff, M.J., *Chapter 11 - Clinical Electromyography*, in *Aminoff's Electrodiagnosis in Clinical Neurology (Sixth Edition)*, M.J. Aminoff, Editor. 2012, W.B. Saunders: London. p. 233-259.
107. Ohno, K., et al., *Choline acetyltransferase mutations cause myasthenic syndrome associated with episodic apnea in humans.* Proc Natl Acad Sci U S A, 2001. **98**(4): p. 2017-22.
108. Kirsch, G.E. and T. Narahashi, *3,4-diaminopyridine. A potent new potassium channel blocker.* Biophys J, 1978. **22**(3): p. 507-12.
109. Cossins, J., et al., *Diverse molecular mechanisms involved in AChR deficiency due to rapsyn mutations.* Brain, 2006. **129**(Pt 10): p. 2773-83.
110. Milone, M., et al., *Myasthenic syndrome due to defects in rapsyn: Clinical and molecular findings in 39 patients.* Neurology, 2009. **73**(3): p. 228-35.
111. Ohno, K., et al., *Rapsyn mutations in humans cause endplate acetylcholine-receptor deficiency and myasthenic syndrome.* Am J Hum Genet, 2002. **70**(4): p. 875-85.
112. Berrih-Aknin, S., M. Frenkian-Cuvelier, and B. Eymard, *Diagnostic and clinical classification of autoimmune myasthenia gravis.* J Autoimmun, 2014. **48-49**: p. 143-8.
113. Carr, A.S., et al., *A systematic review of population based epidemiological studies in Myasthenia Gravis.* BMC Neurol, 2010. **10**: p. 46.
114. Phillips, W.D. and A. Vincent, *Pathogenesis of myasthenia gravis: update on disease types, models, and mechanisms.* F1000Res, 2016. **5**.
115. Vincent, A. and J. Newsom-Davis, *Acetylcholine receptor antibody as a diagnostic test for myasthenia gravis: results in 153 validated cases and 2967 diagnostic assays.* J Neurol Neurosurg Psychiatry, 1985. **48**(12): p. 1246-52.
116. Guptill, J.T., D.B. Sanders, and A. Evoli, *Anti-MuSK antibody myasthenia gravis: clinical findings and response to treatment in two large cohorts.* Muscle Nerve, 2011. **44**(1): p. 36-40.
117. Zisimopoulou, P., et al., *A comprehensive analysis of the epidemiology and clinical characteristics of anti-LRP4 in myasthenia gravis.* J Autoimmun, 2014. **52**: p. 139-45.
118. Lee, J.I. and S. Jander, *Myasthenia gravis: recent advances in immunopathology and therapy.* Expert Rev Neurother, 2017. **17**(3): p. 287-299.
119. Verschuuren, J.J., et al., *Pathophysiology of myasthenia gravis with antibodies to the acetylcholine receptor, muscle-specific kinase and low-density lipoprotein receptor-related protein 4.* Autoimmun Rev, 2013. **12**(9): p. 918-23.

120. Evoli, A., et al., *Clinical correlates with anti-MuSK antibodies in generalized seronegative myasthenia gravis.* Brain, 2003. **126**(Pt 10): p. 2304-11.
121. Conti-Fine, B.M., M. Milani, and H.J. Kaminski, *Myasthenia gravis: past, present, and future.* J Clin Invest, 2006. **116**(11): p. 2843-54.
122. Klooster, R., et al., *Muscle-specific kinase myasthenia gravis IgG4 autoantibodies cause severe neuromuscular junction dysfunction in mice.* Brain, 2012. **135**(Pt 4): p. 1081-101.
123. Punga, A.R., et al., *Muscle-selective synaptic disassembly and reorganization in MuSK antibody positive MG mice.* Exp Neurol, 2011. **230**(2): p. 207-17.
124. Richman, D.P., et al., *Acute severe animal model of anti-muscle-specific kinase myasthenia: combined postsynaptic and presynaptic changes.* Arch Neurol, 2012. **69**(4): p. 453-60.
125. Huijbers, M.G., et al., *MuSK IgG4 autoantibodies cause myasthenia gravis by inhibiting binding between MuSK and Lrp4.* Proc Natl Acad Sci U S A, 2013. **110**(51): p. 20783-8.
126. Shen, C., et al., *Antibodies against low-density lipoprotein receptor-related protein 4 induce myasthenia gravis.* J Clin Invest, 2013. **123**(12): p. 5190-202.
127. Gilhus, N.E. and J.J. Verschuuren, *Myasthenia gravis: subgroup classification and therapeutic strategies.* Lancet Neurol, 2015. **14**(10): p. 1023-36.
128. Punga, A.R. and T. Punga, *Circulating microRNAs as potential biomarkers in myasthenia gravis patients.* Ann N Y Acad Sci, 2018. **1412**(1): p. 33-40.
129. Bartel, D.P., *MicroRNAs: genomics, biogenesis, mechanism, and function.* Cell, 2004. **116**(2): p. 281-97.
130. Lee, E.J., et al., *Systematic evaluation of microRNA processing patterns in tissues, cell lines, and tumors.* Rna, 2008. **14**(1): p. 35-42.
131. Schwarzenbach, H., et al., *Clinical relevance of circulating cell-free microRNAs in cancer.* Nat Rev Clin Oncol, 2014. **11**(3): p. 145-56.
132. Kirschner, M.B., et al., *The Impact of Hemolysis on Cell-Free microRNA Biomarkers.* Front Genet, 2013. **4**: p. 94.
133. Callis, T.E., et al., *Muscling Through the microRNA World.* Experimental Biology and Medicine, 2008. **233**(2): p. 131-138.
134. Horak, M., J. Novak, and J. Bienertova-Vasku, *Muscle-specific microRNAs in skeletal muscle development.* Dev Biol, 2016. **410**(1): p. 1-13.
135. Cheung, T.H., et al., *Maintenance of muscle stem-cell quiescence by microRNA-489.* Nature, 2012. **482**(7386): p. 524-8.
136. Crist, C.G., D. Montarras, and M. Buckingham, *Muscle satellite cells are primed for myogenesis but maintain quiescence with sequestration of Myf5 mRNA targeted by microRNA-31 in mRNP granules.* Cell Stem Cell, 2012. **11**(1): p. 118-26.
137. Chen, J.-F., et al., *microRNA-1 and microRNA-206 regulate skeletal muscle satellite cell proliferation and differentiation by repressing Pax7.* The Journal of Cell Biology, 2010. **190**(5): p. 867-879.
138. Dey, B.K., J. Gagan, and A. Dutta, *miR-206 and -486 induce myoblast differentiation by downregulating Pax7.* Mol Cell Biol, 2011. **31**(1): p. 203-14.
139. Chen, J.F., et al., *The role of microRNA-1 and microRNA-133 in skeletal muscle proliferation and differentiation.* Nat Genet, 2006. **38**(2): p. 228-33.
140. Coletti, D., et al., *Serum Response Factor in Muscle Tissues: From Development to Ageing.* Eur J Transl Myol, 2016. **26**(2): p. 6008.
141. Wei, L., et al., *RhoA signaling via serum response factor plays an obligatory role in myogenic differentiation.* J Biol Chem, 1998. **273**(46): p. 30287-94.

142. Cardinali, B., et al., *Microrna-221 and microrna-222 modulate differentiation and maturation of skeletal muscle cells.* PLoS One, 2009. **4**(10): p. e7607.
143. Nakasa, T., et al., *Acceleration of muscle regeneration by local injection of muscle-specific microRNAs in rat skeletal muscle injury model.* J Cell Mol Med, 2010. **14**(10): p. 2495-505.
144. Valadi, H., et al., *Exosome-mediated transfer of mRNAs and microRNAs is a novel mechanism of genetic exchange between cells.* Nat Cell Biol, 2007. **9**(6): p. 654-9.
145. Cacchiarelli, D., et al., *miRNAs as serum biomarkers for Duchenne muscular dystrophy.* EMBO Mol Med, 2011. **3**(5): p. 258-65.
146. Jeanson-Leh, L., et al., *Serum profiling identifies novel muscle miRNA and cardiomyopathy-related miRNA biomarkers in Golden Retriever muscular dystrophy dogs and Duchenne muscular dystrophy patients.* Am J Pathol, 2014. **184**(11): p. 2885-98.
147. Punga, T., et al., *Circulating miRNAs in myasthenia gravis: miR-150-5p as a new potential biomarker.* Ann Clin Transl Neurol, 2014. **1**(1): p. 49-58.
148. Molin, C.J., et al., *Thymectomy lowers the myasthenia gravis biomarker miR-150-5p.* Neurol Neuroimmunol Neuroinflamm, 2018. **5**(3): p. e450.
149. Punga, T., et al., *Disease specific enrichment of circulating let-7 family microRNA in MuSK+ myasthenia gravis.* J Neuroimmunol, 2016. **292**: p. 21-6.
150. Liu, J., et al., *Current Methods for Skeletal Muscle Tissue Repair and Regeneration.* BioMed research international, 2018. **2018**: p. 1984879-1984879.
151. Bursac, N., M. Juhas, and T.A. Rando, *Synergizing Engineering and Biology to Treat and Model Skeletal Muscle Injury and Disease.* Annu Rev Biomed Eng, 2015. **17**: p. 217-42.
152. Gibbons, M.C., M.A. Foley, and K.O. Cardinal, *Thinking inside the box: keeping tissue-engineered constructs in vitro for use as preclinical models.* Tissue Eng Part B Rev, 2013. **19**(1): p. 14-30.
153. Ikeda, K., et al., *In vitro drug testing based on contractile activity of C2C12 cells in an epigenetic drug model.* Scientific Reports, 2017. **7**: p. 44570.
154. Vandenburgh, H., et al., *Automated drug screening with contractile muscle tissue engineered from dystrophic myoblasts.* Faseb j, 2009. **23**(10): p. 3325-34.
155. Sharples, A.P., et al., *Modelling in vivo skeletal muscle ageing in vitro using three-dimensional bioengineered constructs.* Aging Cell, 2012. **11**(6): p. 986-95.
156. Delaporte, C., B. Dautreaux, and M. Fardeau, *Human myotube differentiation in vitro in different culture conditions.* Biol Cell, 1986. **57**(1): p. 17-22.
157. Kobayashi, T. and V. Askanas, *Acetylcholine receptors and acetylcholinesterase accumulate at the nerve-muscle contacts of de novo grown human monolayer muscle cocultured with fetal rat spinal cord.* Exp Neurol, 1985. **88**(2): p. 327-35.
158. Askanas, V., et al., *De novo neuromuscular junction formation on human muscle fibres cultured in monolayer and innervated by foetal rat spinal cord: ultrastructural and ultrastructural--cytochemical studies.* J Neurocytol, 1987. **16**(4): p. 523-37.
159. Kobayashi, T., V. Askanas, and W.K. Engel, *Human muscle cultured in monolayer and cocultured with fetal rat spinal cord: importance of dorsal root ganglia for achieving successful functional innervation.* J Neurosci, 1987. **7**(10): p. 3131-41.

160. Sytkowski, A.J., Z. Vogel, and M.W. Nirenberg, *Development of acetylcholine receptor clusters on cultured muscle cells.* Proc Natl Acad Sci U S A, 1973. **70**(1): p. 270-4.
161. Axelrod, D., et al., *Lateral motion of fluorescently labeled acetylcholine receptors in membranes of developing muscle fibers.* Proc Natl Acad Sci U S A, 1976. **73**(12): p. 4594-8.
162. Christian, C.N., et al., *A factor from neurons increases the number of acetylcholine receptor aggregates on cultured muscle cells.* Proc Natl Acad Sci U S A, 1978. **75**(8): p. 4011-5.
163. Kummer, T.T., et al., *Nerve-independent formation of a topologically complex postsynaptic apparatus.* J Cell Biol, 2004. **164**(7): p. 1077-87.
164. Streit, J., *Mechanisms of pattern generation in co-cultures of embryonic spinal cord and skeletal muscle.* Int J Dev Neurosci, 1996. **14**(2): p. 137-48.
165. Blau, H.M., C.-P. Chiu, and C. Webster, *Cytoplasmic activation of human nuclear genes in stable heterocaryons.* Cell, 1983. **32**(4): p. 1171-1180.
166. Yaffe, D. and O.R.A. Saxel, *Serial passaging and differentiation of myogenic cells isolated from dystrophic mouse muscle.* Nature, 1977. **270**(5639): p. 725-727.
167. Casas-Delucchi, C.S., et al., *Histone acetylation controls the inactive X chromosome replication dynamics.* Nat Commun, 2011. **2**: p. 222.
168. Tannu, N.S., et al., *Comparative proteomes of the proliferating C(2)C(12) myoblasts and fully differentiated myotubes reveal the complexity of the skeletal muscle differentiation program.* Mol Cell Proteomics, 2004. **3**(11): p. 1065-82.
169. Rajan, S., et al., *Analysis of early C2C12 myogenesis identifies stably and differentially expressed transcriptional regulators whose knock-down inhibits myoblast differentiation.* Physiol Genomics, 2012. **44**(2): p. 183-97.
170. Chen, J.-F., et al., *The role of microRNA-1 and microRNA-133 in skeletal muscle proliferation and differentiation.* Nature Genetics, 2006. **38**(2): p. 228-233.
171. Lorenzon, P., et al., *Spontaneous and repetitive calcium transients in C2C12 mouse myotubes during in vitro myogenesis.* Eur J Neurosci, 1997. **9**(4): p. 800-8.
172. McMahon, D.K., et al., *C2C12 cells: biophysical, biochemical, and immunocytochemical properties.* Am J Physiol, 1994. **266**(6 Pt 1): p. C1795-802.
173. Engler, A.J., et al., *Myotubes differentiate optimally on substrates with tissue-like stiffness: pathological implications for soft or stiff microenvironments.* J Cell Biol, 2004. **166**(6): p. 877-887.
174. Huang, N.F., et al., *Myotube assembly on nanofibrous and micropatterned polymers.* Nano letters, 2006. **6**(3): p. 537-542.
175. Deshmukh, A.S., et al., *Deep proteomics of mouse skeletal muscle enables quantitation of protein isoforms, metabolic pathways, and transcription factors.* Molecular & Cellular Proteomics, 2015. **14**(4): p. 841-853.
176. Hosseini, V., et al., *Engineered contractile skeletal muscle tissue on a microgrooved methacrylated gelatin substrate.* Tissue Engineering Part A, 2012. **18**(23-24): p. 2453-2465.
177. Mantegazza, R., et al., *Animal models of myasthenia gravis: utility and limitations.* Int J Gen Med, 2016. **9**: p. 53-64.
178. Baggi, F., et al., *Acetylcholine receptor-induced experimental myasthenia gravis: what have we learned from animal models after three decades?* Arch Immunol Ther Exp (Warsz), 2012. **60**(1): p. 19-30.

179. Guo, X., et al., *Neuromuscular junction formation between human stem cell-derived motoneurons and human skeletal muscle in a defined system.* Biomaterials, 2011. **32**(36): p. 9602-11.
180. Taylor, A.M., et al., *A microfluidic culture platform for CNS axonal injury, regeneration and transport.* Nat Methods, 2005. **2**(8): p. 599-605.
181. Southam, K.A., et al., *Microfluidic primary culture model of the lower motor neuron-neuromuscular junction circuit.* J Neurosci Methods, 2013. **218**(2): p. 164-9.
182. Thomas, C.A., Jr., et al., *A miniature microelectrode array to monitor the bioelectric activity of cultured cells.* Exp Cell Res, 1972. **74**(1): p. 61-6.
183. Ballini, M., et al., *A 1024-Channel CMOS Microelectrode Array With 26,400 Electrodes for Recording and Stimulation of Electrogenic Cells In Vitro.* IEEE J Solid-State Circuits, 2014. **49**(11): p. 2705-2719.
184. Radivojevic, M., et al., *Tracking individual action potentials throughout mammalian axonal arbors.* Elife, 2017. **6**.
185. Lewandowska, M.K., et al., *Cortical Axons, Isolated in Channels, Display Activity-Dependent Signal Modulation as a Result of Targeted Stimulation.* Front Neurosci, 2016. **10**: p. 83.
186. Lewandowska, M.K., et al., *Recording large extracellular spikes in microchannels along many axonal sites from individual neurons.* PLoS One, 2015. **10**(3): p. e0118514.
187. Ballini, M., et al., *A 1024-Channel CMOS microelectrode array with 26,400 electrodes for recording and stimulation of electrogenic cells in vitro.* Solid-State Circuits, IEEE Journal of, 2014. **49**(11): p. 2705-2719.
188. Schmittgen, T.D. and K.J. Livak, *Analyzing real-time PCR data by the comparative C(T) method.* Nat Protoc, 2008. **3**(6): p. 1101-8.
189. Inturi, R., S. Thaduri, and T. Punga, *Adenovirus precursor pVII protein stability is regulated by its propeptide sequence.* PLoS One, 2013. **8**(11): p. e80617.
190. Rabieh, N., et al., *On-chip, multisite extracellular and intracellular recordings from primary cultured skeletal myotubes.* Scientific Reports, 2016. **6**: p. 36498.
191. Nag, A.C. and J.D. Foster, *Myogenesis in adult mammalian skeletal muscle in vitro.* J Anat, 1981. **132**(Pt 1): p. 1-18.
192. Pogogeff, I.A. and M.R. Murray, *Form and behavior of adult mammalian skeletal muscle in vitro.* Anat Rec, 1946. **95**: p. 321-35.
193. Sciancalepore, M., et al., *Intrinsic ionic conductances mediate the spontaneous electrical activity of cultured mouse myotubes.* Biochimica et Biophysica Acta (BBA)-Biomembranes, 2005. **1720**(1): p. 117-124.
194. Bandi, E., et al., *Autocrine activation of nicotinic acetylcholine receptors contributes to Ca2+ spikes in mouse myotubes during myogenesis.* The Journal of physiology, 2005. **568**(1): p. 171-180.
195. Stalberg, E., J. Ekstedt, and A. Broman, *Neuromuscular transmission in myasthenia gravis studied with single fibre electromyography.* J Neurol Neurosurg Psychiatry, 1974. **37**(5): p. 540-7.
196. Ashby, P.R., S.J. Wilson, and A.J. Harris, *Formation of primary and secondary myotubes in aneural muscles in the mouse mutant peroneal muscular atrophy.* Dev Biol, 1993. **156**(2): p. 519-28.
197. Wilson, S.J. and A.J. Harris, *Formation of myotubes in aneural rat muscles.* Dev Biol, 1993. **156**(2): p. 509-18.
198. Condon, K., et al., *Differentiation of fiber types in aneural musculature of the prenatal rat hindlimb.* Dev Biol, 1990. **138**(2): p. 275-95.

199. Punga, A., *Myasthenia Gravis: New Insights into the Effect of MuSK Antibodies and Acetylcholinesterase Inhibitors*. 2011.
200. Mori, S., et al., *Antibodies against Muscle-Specific Kinase Impair Both Presynaptic and Postsynaptic Functions in a Murine Model of Myasthenia Gravis*. The American Journal of Pathology, 2012. **180**(2): p. 798-810.
201. Sjøholt, G., et al., *Genomic Structure and Chromosomal Localization of a Humanmyo-Inositol Monophosphatase Gene (IMPA)*. Genomics, 1997. **45**(1): p. 113-122.
202. Sjoholt, G., et al., *Examination of IMPA1 and IMPA2 genes in manic-depressive patients: association between IMPA2 promoter polymorphisms and bipolar disorder*. Mol Psychiatry, 2004. **9**(6): p. 621-9.
203. Wittbrodt, E.T., *Drugs and Myasthenia Gravis: An Update*. JAMA Internal Medicine, 1997. **157**(4): p. 399-408.
204. Ozkok, E., et al., *Reduced muscle mitochondrial enzyme activity in MuSK-immunized mice*. Clin Neuropathol, 2015. **34**(6): p. 359-63.
205. Zalewska, E. and I. Hausmanowa-Petrusewicz, *Correlating motor unit morphology with bioelectrical activity - A simulation study*. Clin Neurophysiol, 2018. **129**(1): p. 271-279.
206. Jones, R.A., et al., *NMJ-morph reveals principal components of synaptic morphology influencing structure–function relationships at the neuromuscular junction*. Open Biology, 2016. **6**(12): p. 160240.
207. Entwistle, A., et al., *The control of chick myoblast fusion by ion channels operated by prostaglandins and acetylcholine*. J Cell Biol, 1988. **106**(5): p. 1693-702.
208. Krause, R.M., et al., *Activation of nicotinic acetylcholine receptors increases the rate of fusion of cultured human myoblasts*. J Physiol, 1995. **489 (Pt 3)**: p. 779-90.
209. Valenzuela, D.M., et al., *Receptor tyrosine kinase specific for the skeletal muscle lineage: expression in embryonic muscle, at the neuromuscular junction, and after injury*. Neuron, 1995. **15**(3): p. 573-84.
210. Bandi, E., et al., *Autocrine activation of nicotinic acetylcholine receptors contributes to Ca2+ spikes in mouse myotubes during myogenesis*. J Physiol, 2005. **568**(Pt 1): p. 171-80.
211. Bezakova, G., et al., *Neural agrin controls acetylcholine receptor stability in skeletal muscle fibers*. Proc Natl Acad Sci U S A, 2001. **98**(17): p. 9924-9.
212. Morsch, M., et al., *Muscle specific kinase autoantibodies cause synaptic failure through progressive wastage of postsynaptic acetylcholine receptors*. Experimental Neurology, 2012. **237**(2): p. 286-295.

Acta Universitatis Upsaliensis

Digital Comprehensive Summaries of Uppsala Dissertations from the Faculty of Medicine 1607

Editor: The Dean of the Faculty of Medicine

A doctoral dissertation from the Faculty of Medicine, Uppsala University, is usually a summary of a number of papers. A few copies of the complete dissertation are kept at major Swedish research libraries, while the summary alone is distributed internationally through the series Digital Comprehensive Summaries of Uppsala Dissertations from the Faculty of Medicine. (Prior to January, 2005, the series was published under the title "Comprehensive Summaries of Uppsala Dissertations from the Faculty of Medicine".)

Distribution: publications.uu.se
urn:nbn:se:uu:diva-395581

ACTA
UNIVERSITATIS
UPSALIENSIS
UPPSALA
2019